DESIGN OF A SIX DEGREE-OF-FREEDOM HAPTIC HYBRID PLATFORM MANIPULATOR

A Thesis Submitted to
the Graduate School of Engineering and Sciences of
İzmir Institute of Technology
in Partial Fulfillment of the Requirements for the Degree of

MASTER OF SCIENCE

in Mechanical Engineering

by
TUNÇ BİLGİNCAN

May 2010
İZMİR

We approve the thesis of **Tunç BİLGİNCAN**

Assist.Prof. Dr. Mehmet İsmet Can DEDE
Supervisor

Prof. Dr. Tech. Sc. Rasim ALİZADE
Committee Member

Assist. Prof. Dr. Enver TATLICIOĞLU
Committee Member

11 May 2010

Prof. Dr. Metin TANOĞLU
Head of the Department of
Mechanical Engineering

Assoc. Prof. Dr. Talat YALÇIN
Dean of the Graduate School
of Engineering and Sciences

ACKNOWLEDGEMENTS

In the first place, I would like to thank my advisor Assist. Prof. Dr. Mehmet Ismet Can DEDE for his guidance and valuable knowledge during my MSC study. I wish to express sincere appreciation to my committee members Prof. Dr. Tech. Sc. Rasim ALİZADE, and Assist. Prof. Dr. Enver TATLICIOĞLU for their comments and advices.

I also would like to thank the members of the mechatronics laboratory, Erkin GEZGİN and Özgün SELVİ for their help and support. I am very grateful to my friends, Erman AYTAR, Ali KARA and Cenk KILIÇASLAN for their friendship.

Most importantly, I owe gratefulness to my family for their good wishes and prayers. I send special thanks to İA for her supports and patience.

This research was supported by a Marie Curie International Reintegration Grant within the 7th European Community Framework Programme.

ABSTRACT

DESIGN OF A SIX DEGREE-OF-FREEDOM HAPTIC HYBRID PLATFORM MANIPULATOR

The word Haptic, based on an ancient Greek word called haptios, means related with touch. As an area of robotics, haptics technology provides the sense of touch for robotic applications that involve interaction with human operator and the environment. The sense of touch accompanied with the visual feedback is enough to gather most of the information about a certain environment. It increases the precision of teleoperation and sensation levels of the virtual reality (VR) applications by exerting physical properties of the environment such as forces, motions, textures. Currently, haptic devices find use in many VR and teleoperation applications.

The objective of this thesis is to design a novel Six Degree-of-Freedom (DOF) haptic desktop device with a new structure that has the potential to increase the precision in the haptics technology. First, previously developed haptic devices and manipulator structures are reviewed. Following this, the conceptual designs are formed and a hybrid structured haptic device is designed manufactured and tested.

Developed haptic device's control algorithm and VR application is developed in Matlab© Simulink. Integration of the mechanism with mechanical, electro-mechanical and electronic components and the initial tests of the system are executed and the results are presented. According to the results, performance of the developed device is discussed and future works are addressed.

ÖZET

ALTI SERBESTLİK DERECELİ HAPTİK HİBRİT PLATFORM MANİPÜLATÖRÜ TASARIMI

Haptik kelimesi antik Yunancada haptios olarak geçmekte ve dokunma duyusuyla ilgili anlamına gelmektedir. Robotiğin bir uygulama alanı olan haptik cihazlar, robotik uygulamalara dokunma duyusunu eklemekte ve kullanıcı ile olan etkileşimi artırmaktadır. Görsel duyu ile birlikte dokunma duyusu, çoğu zaman bulunduğumuz ortamı anlamamız için yeterli olan bilgiyi sağlayabilmektedir. Haptik cihazlar bulunulan ortama ait kuvvet, hareket, yüzey yapısı gibi fiziksel öğeleri kullanıcıya ileterek uzaktan kumanda işlerinde yapılan işin hassasiyetini ve sanal gerçeklik uygulamalarında sanal gerçekliği artırmaktadır. Günümüzde haptik cihazlar birçok sanal gerçeklik ve uzaktan kumanda işlerinde kullanılmaktadır.

Bu tezin amacı, günümüzde haptik teknolojinin sahip olduğu hassasiyeti artırabilecek potansiyele sahip 6 serbestlik dereceli özgün yapıda bir masaüstü haptik cihazı geliştirmektir. Öncelikle bu amaçla mevcut bulunan haptik cihazlar ve mekanizmalar incelenmiştir. Sonrasında kavramsal tasarımlar oluşturulmuş ve hibrit yapıda haptik cihaz tasarlanmış, üretilmiş ve test edilmiştir.

Geliştirilen haptik cihazın kontrol algoritması ve sanal gerçeklik uygulaması Matlab© Simulink' te oluşturulmuş. Sistemin ilk denemeleri mekanik, elektromekanik ve elektronik kısımları ile birleştirilmesinden sonra gerçekleştirilmiş ve geliştirilen cihazdan alınan sonuçlar tartışılmış ve gelecekte yapılması hedeflenen çalışmalar önerilmiştir.

TABLE OF CONTENTS

LIST OF FIGURES

Figure **Page**

LIST OF TABLES

Table **Page**

LIST OF SYMBOLS

R	Revolute joint
P	Prismatic joint
S	Spherical joint
Sl	Sliding joint
θ_i	Rotation angle of the first links of the translation mechanism
l_i	Link lengths of the translation mechanism
S_i	Workspace location identification parameter
Wr	Point of interest of the translation mechanism (Wrist point)
O	Origin point
C	Rotation sequence
α	First rotation angle for isometric projection
β	Second rotation angle for isometric projection
σ	Sign ambiguity
F	Applied force
T_i	Applied torque

CHAPTER 1

INTRODUCTION

1.1. The Senses and the Sense of Touch

The brain is the center of the nervous system that understands ideas, performs mental tasks, manipulates our body functions and provides awareness of our surroundings. The fact of awareness and understanding the surrounding starts with the sensation and the sensation begins with sensory reception by sensory receptors. Sensory receptors are specified cells that respond to specific changes in the environment.

Five senses are an evolution of specialized sensory receptors located in specific locations in the human body. Basically, human beings have five senses, vision (sight), audition (hearing), olfaction (smell), gustation (taste) and somatosense (touch). These senses provide connection between the physical world and human brain.

Receptors that respond to light energy are known as photoreceptors allocated in the retina of the eye. In many respects, the basic imaging principle of the eye is similar to digital cameras with an adjustable iris and retina. Vision is a unique sense that provides us to see the world and it possesses a great potential to perceive most of the required stimuli originated from the environment. The sense of hearing allows us to detect sound waves and interpret them to the electro-chemical pulses. Sound is audible vibrations of air molecules and ear is an electro-mechanical organ that detects these acoustic vibrations. It provides us auditory feedback from the environment. This sense is necessary for hearing and speech for communication and the basis of social interactions. Gustation, the sense of taste, is accomplished by chemoreceptors that respond to chemicals dissolved in our mouths. Gustation provides information about the quality of the food and liquid which is important both for psychological and physical health. The sense of smell is acquired by chemoreceptors that respond to chemicals in air. Also it has importance for psychological and physical health.

Among all senses, touch sense is the most amazing and necessary one. In embryos, it develops and activates before all other senses. It is the most simple and

most improved sense that provides interaction with the environment. It provides information about texture, shape, temperature, weight, etc. of an object or environment. Touch sense is the most durable sense organ because it employs many connections to nervous system from every single part of the body. This complexity also provides reliable sensory inputs to cerebral cortex of the brain. Basically the mechanoreceptors can be classified into two groups based on the location in the body. Kinaesthetic receptors are located in muscles, tendons and joints of the body and cutaneous receptors located in the skin. Nowadays, haptics technology is developing to stimulate both of these systems.

Outlined five senses are our connection to world around us and human-computer interfaces are the equipments that are designed to provide interaction between our brains and the computer via our senses. In the beginning of the development of computers, human-computer interaction is provided with visual feedback technologies such as monitors. Afterwards auditory technologies are developed and improved the interaction levels. Although the sense of touch has a great potential to increase the human and computer interaction, due to the limitations of the data process capabilities and transfer rates, the first human and computer interaction applications were bounded by visual and auditory technologies. However, today it is clear that the sense of touch is essential for high level human and computer interaction to improve the perception of the environment. Today, powerful microprocessor and computer technology allows us to process such high amount of data thus makes haptics technology available for various implementations.

Currently haptic devices are reality and many haptic systems are effectively used for a wide variety of applications such as computer aided design, entertainment, education, training, rehabilitation, nano-manipulation, molecular technology, virtual prototyping and virtual sculpturing.

1.2. Objective of the Thesis

The sense of touch is a viable feedback to understand the environment. Most of the time, the sense of touch accompanied with the visual feedback is enough to gather most of the information about a certain environment. Therefore various types of haptic devices are developed, and they are employed in different types of tasks. Especially for

accurate teleoperation and high level VR applications, high precision haptic systems are required with respect to the current commercially available haptic devices. In order to meet this precision criterion, in this thesis, 6-DOF high precision desktop haptic device is designed and manufactured. It is also aimed to design, custom data acquisition (DAQ) system for the manufactured mechanism. Therefore previous data acquisition designs investigated for such applications.

The final aim of this work is to employ the developed system in a VR application for the performance tests of system and finalize the system to be ready for future teleoperation applications.

1.3. Outline

The following Chapter provides three different sections for haptic devices classification that are grouped by their haptic sensation types, mechanism types and applications. Each category is explained with several examples.

The fundamentals and basic components of a haptic device design are described in Chapter 3. The components of the mechanical, electro-mechanical and electronics parts are listed and discussed. The importance of the material selection in haptic device design is explained and conventional haptic drive systems are shown with examples. Electromechanical components such as sensors and actuators are described and previously used components are presented. Commercial and custom data acquisition systems and motor amplifiers are compared and computer control interface of a haptic device are discussed.

Chapter 4, is dedicated to design, analysis and simulations of the mechanism. The design criteria are listed and discussed, the design procedure is presented both for translation and orientation mechanism. The CAD analysis results via SolidWorks© CosmosMotion© (a CAD and mechanism analysis software) are discussed. Kinematic analysis for the mechanism is also presented in this chapter.

The manufacturing processes of the mechanism are explained in Chapter 5. Material selection criteria are provided and the manufacturing processes of all parts are explained in detail.

In Chapter 6, the integration of the mechanical, electro-mechanical and electronic components are presented. The part selection and integration of the complete system is described. Experimental results are provided and discussed.

In conclusion part, conclusions and findings explained. The future modifications in the mechanism are proposed. The possible future applications of the system are listed.

CHAPTER 2

BACKGROUND

2.1. Introduction

Wide variety of types and sizes of haptic devices are utilized in various state-of-the-art applications for both scientific and commercial purposes. Haptics technology is usually used for complex tasks such as controlling a manipulator in hazardous environments, minimal invasive surgery, robotic rehabilitation, nano manipulation task, 3D design, education and training applications.

In this chapter, the aim is to describe previous haptic applications and clarify the concept of haptics. In order to achieve this objective haptics technology is investigated in three separate groups by their: (1) feedback types, (2) mechanical structures, and (3) applications.

2.2. Kinaesthetic and Cutaneous Haptic Devices

Kinaesthetic receptors are located in muscles, tendons and joints of the body as shown in Figure 2.1(a). The kinaesthetic system refers to the awareness of force, motion, position and low frequency vibration. Cutaneous receptors are located in the dermis and epidermis layer of skin as shown in Figure 2.1(b). Cutaneous system refers to the awareness of touch, pressure, stretch, texture and high frequency vibration.

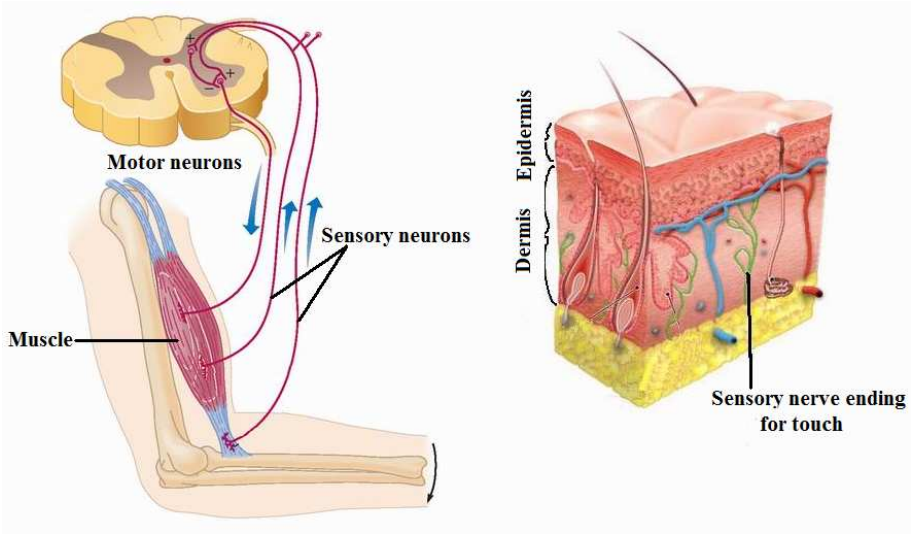

(a) (b)

Figure 2.1. Types of mechanoreceptors receptors: (a) Kinaesthetic, (b) Cutaneous (Source: Medical-look 2010)

2.2.1. Kinaesthetic Haptic Devices

Kinaesthetic display devices are human–computer interfaces that can simulate kinaesthetic parameters of an environment or an object, such as motion, location, weight and rigidity. Recently, kinaesthetic haptic devices are the most common type of haptic interfaces. Several types of robot arm mechanisms have already been configured as kinaesthetic haptic devices. However, it is still an active field of research and development.

Wearable haptic devices are the most common example for kinaesthetic haptic devices. Skeletal representation and actual picture of a wearable haptic system for the arm is shown in Figure 2.2(a) and Figure 2.2(b). The mechanism was developed to fit the human body with an Electromyography (EMG) based force representation (Sone, et al. 2008).

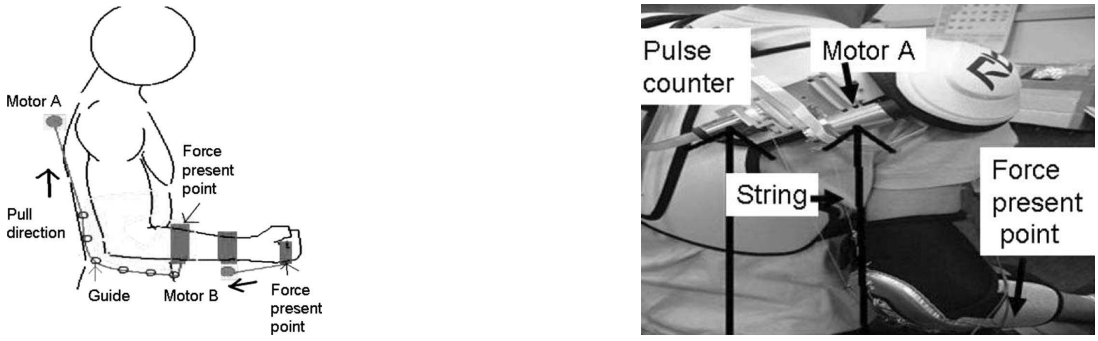

(a) (b)

Figure 2.2. Wearable haptic application for arm: (a) Representation, (b) Actual (Source: Sone, et al. 2008)

A haptic interface for the thumb and index fingers of the user can be seen in Figure 2.3 that stimulates a two point contact (Frisoli, et al. 2007).

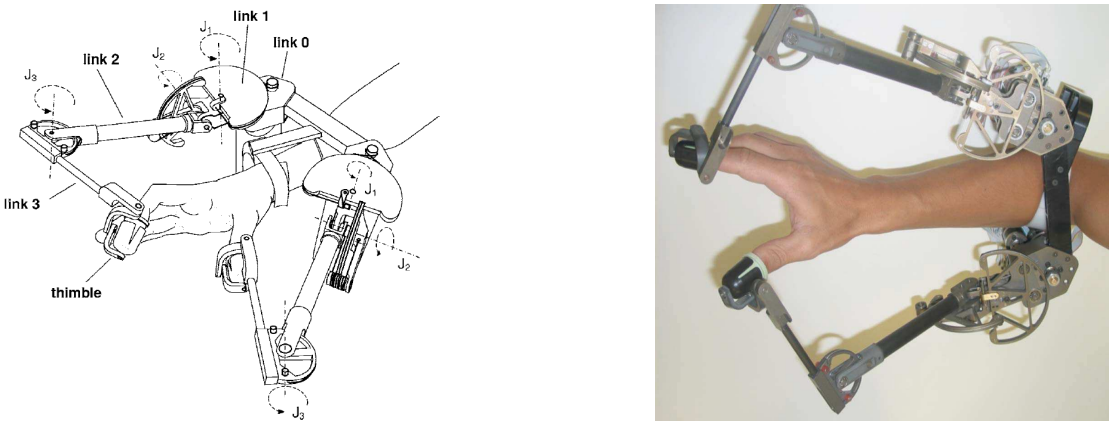

(a) (b)

Figure 2.3. Wearable haptic application for hand: (a) Representation, (b) Actual (Source: Frisoli, et al. 2007)

Representation of a planar 4 wire driven 3-DOF haptic interface with a circular end-effector is shown in Figure 2.4. Planar mechanism can provide forces about $\vec{u}_1$ and $\vec{u}_2$ axes and moment about $\vec{u}_3$ axis. The system has relatively large workspace and easy kinematic analysis which was presented in Paolo Gallina and G. Rosati. (Gallina and Rosati 2002).

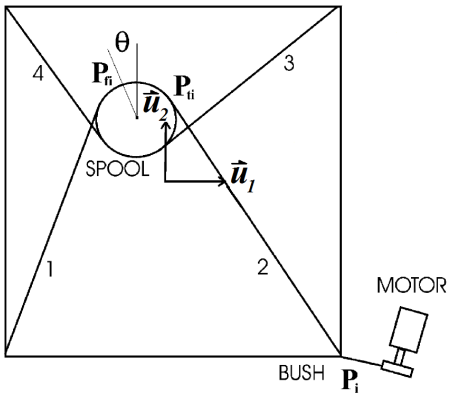

Figure 2.4. Representation of 4 wire haptic interface
(Source: Gallina and Rosati 2002)

In Figure 2.5 prototype of a novel parallel haptic device is shown. The kinematic structure of the mechanism is based on a well-known Delta manipulator. The structure is arranged in a special configuration. The two rotary actuators are placed on the same direction and the other actuator is placed perpendicular to the direction of the other actuators. This provides high stiffness and enlarged workspace. The stiffness and kinematic analysis have been performed and the design was optimized to maximize the stiffness and to increase the workspace (Kim, et al. 2007).

Figure 2.5. Prototype of 3-DOF parallel-type haptic device
(Source: Kim, et al. 2007)

2.2.2. Cutaneous Haptic Devices

Cutaneous display devices are human–computer interfaces that can copy tactile parameters of a surface such as texture, shape, roughness and temperature. Cutaneous device technology has been developed making use of several technologies such as mechanical needles actuated by electro-magnetics, piezoelectric materials, shape memory alloys and pneumatics.

The cutaneous sensation is not only an area of haptics technology it has also several applications in nature. The behaviour of antenna was studied in blinded American cockroaches. The antenna of an insect has both cutaneous and kinaesthetic sensor behaviour (Okada and Toh 2004).

An example for such an inspiration from the biological systems is the Garcia robot shown in Figure 2.6. It has bio-inspired tactile sensors and programmed for high-speed wall following task (Lee, et al. 2008).

Figure 2.6. Garcia robot with embedded flex sensors and antenna
(Source: Lee, et al. 2008)

As it was previously outlined, haptics has a wide range of application field in minimal invasive surgery applications. The importance of force and tactile feedback for surgeries was outlined and a review of artificial tactile feedback in laparoscopic surgery presented by Schostek, et al (Schostek, et al. 2009).

Various types of tactile display devices and tactile actuation systems are still an active research area. A tactile display device called VITAL1 is shown in Figure2.7. It has an 8x8 arranged pin matrix that is actuated by electro-magnetic actuators (Benali-Khoudja, et al. 2007).

Figure 2.7. VITAL1: vibrotactile display
(Source: Benali-Khoudja, et al. 2007)

2.2.3. Combination of Kinaesthetic and Cutaneous Haptic Devices

Combination of kinaesthetic and cutaneous sensation in one haptic device improves realistic hand and object interaction between user and computer. Currently most of the developed haptic interfaces are separated as, force feedback devices and tactile devices. Nevertheless some combined haptic systems that have the capability to stimulate both kinaesthetic and cutaneous receptors.

A pen-like haptic interface is shown in Figure 2.8. The system is based on a tactile display and a vibrating module. It is also combined with PHANTOM^{TM} haptic system in order to add kinaesthetic feedback capabilities to the pen-like haptic interface (Kyung, et al. 2007).

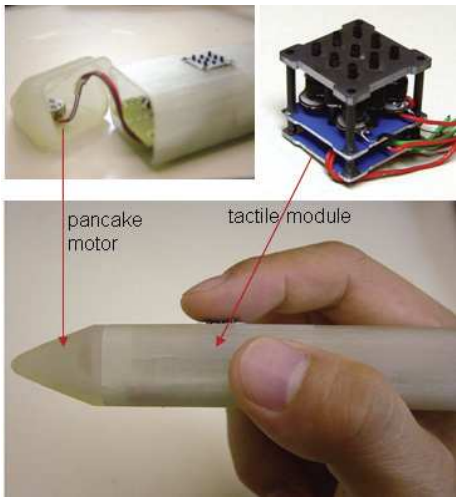

Figure 2.8. Prototype of a pen-like Haptic Interface
(Source: Kyung, et al. 2007)

2.3. Haptic Device Mechanisms

Serial manipulators are the most common industrial robots that have been widely used variety of applications. They have serial mechanical arm structure, which is a composition of serial chain of links and joints. The main advantage of the serial manipulators is their large workspace with respect to their footprint. However their low stiffness, amplified errors from link to link due to their open kinematic structure are their main disadvantages. The serial structure has to carry and move the large weights of links and the actuators; hence it has limited loading capacities.

A parallel manipulator is a closed-loop mechanism with an end-effector placed on the moving platform that is connected to the ground with kinematic chains. Parallel manipulators have some structural advantages with respect to serial manipulators such as their higher precision, robustness and stiffness. The mechanism has to carry relatively low mass due to its ground fixed actuators. Therefore parallel manipulators have higher loading capacity with respect to the serial manipulators. Their major disadvantage is their limited workspace, and low stiffness in singular positions.

A Hybrid manipulator is a combination of parallel and serial manipulators. They embrace the advantages of both serial and parallel manipulators.

2.3.1. Serial Mechanisms

Serial structures have been used in many haptic interface designs. Serial structure haptic devices are commercially available and probably the most well known devices are the products of Sensable Technologies (www.sensable.com 2010). The PHANTOM haptic device is currently used in various types of applications that range from commercial to scientific purposes. 6-DOF portable PHANTOM Desktop Haptic Device can apply 1.75 N continuous exertable forces about $\vec{u}_1$, $\vec{u}_2$, $\vec{u}_3$ axes and it has also 3 passive rotational axes for sensing the rotational motions (Figure 2.9) (Massie and Salibury 1994).

Figure 2.9. PHANTOM® Desktop™ Haptic Device
(Source: Sensable 2010)

Other products of Sensable Technologies can be seen in Figure 2.10. PHANTOM 1.5/6-DOF and PHANTOM 3.0/6-DOF have higher translational force feedback capabilities with respect to the previously shown haptic devices. 1.5 HIGH FORCE/6-DOF HAPTIC DEVICE has 3N continuous exertable force about $\vec{u}_1$, $\vec{u}_2$, $\vec{u}_3$ axes and also they are capable of providing torque feedback for rotational motions.

(a) (b)

Figure 2.10. Some products of Sensable (a) PHANTOM 1.5, (b) PHANTOM 3.0
(Source: Sensable 2010)

Several types of special purpose serial structure haptic interfaces were also developed. 2-DOF haptic joystick for PC video games is shown in Figure 2.11. The system is based on gimbal structure with two actuators and potentiometers (Kyihwan Park, et al. 2004).

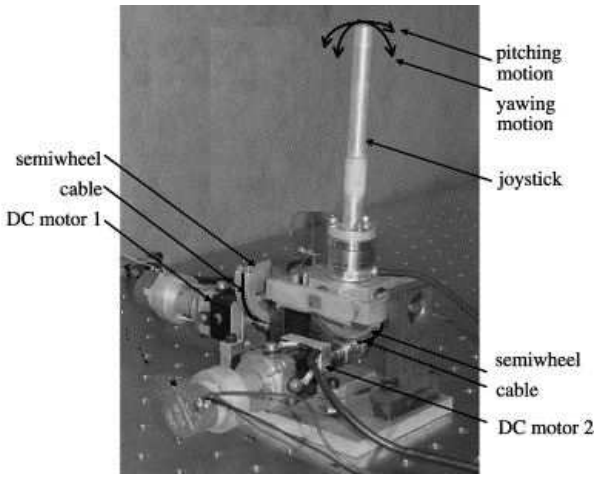

Figure 2.11. 2-DOF Haptic joystick
(Source: Park, et al. 2004)

Wearable haptic interfaces are usually designed in serial structure in order to fit the mechanism to human body. A 4-DOF portable haptic interface can be seen in Figure 2.12. The device is designed for the index finger and it has passive force feedback capability utilizing mechanical brakes (Lelieveld and Maeno 2006).

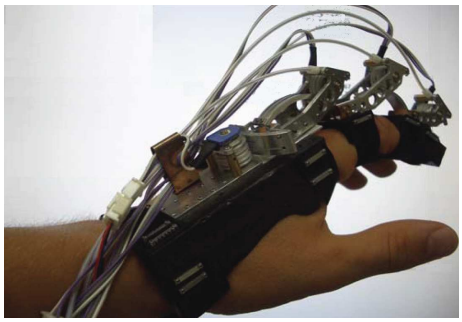

Figure 2.12. Force feedback for the index finger
(Source: Lelieveld and Maeno 2006)

Wearable exoskeleton haptic interfaces are frequently used as rehabilitation systems. An example for such an application is the wearable haptic interface shown in Figure 2.13. The Maryland-Georgetown-Army (MGA) Exoskeleton has 6-DOF and it is designed and developed for shoulder rehabilitation applications (Carignan, et al. 2009).

Figure 2.13. The MGA Exoskeleton
(Source: Carignan, et al. 2009)

Haptics technology is also used for medical purposes. A training simulator mechanism for urological operations is shown in Figure 2.14. The 5-DOF mechanism is designed to reproduce even very small forces and moments; hence it has low mass and inertia (Vlachos and Papadopoulos 2003).

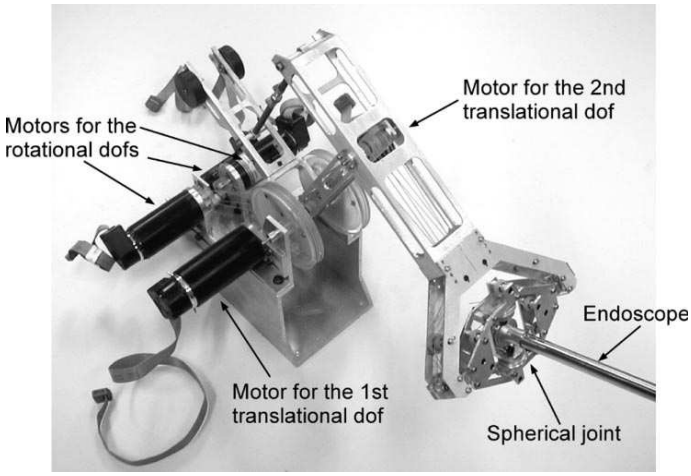

Figure 2.14. 5-DOF simulator for urological operations
(Source: Vlachos and Papadopoulos 2003)

2.3.2. Parallel Mechanisms

Various researchers have recently designed several types of parallel structure haptic interfaces. Most of the published designs in the literature are based on delta structure.

Figure 2.15. 6 URS Haptic Device
(Source: Sabater, et al. 2004)

In Figure 2.15, a modified version of Gough–Steward platform is configured as 6-DOF parallel haptic device. The system has cable-driven pantographs and rotational electrical actuators for improved workspace and output bandwidth (Sabater, et al. 2004).

A 7-DOF haptic device called PATHOS II was designed and manufactured by Keehoon Kim et al. 6-DOF of the device is reserved for the spatial manipulation and the remaining 1-DOF for grasping the objects. The parallel mechanism design was chosen to enhance the stiffness and accuracy. Their experimental results indicated that the mechanism can display virtual environment with some stiffness and accuracy (Kim, et al. 2003).

6-DOF haptic mechanism, shown in Figure 2.16, is a combination of a 3-DOF planar lower parallel mechanism and another 3-DOF parallel mechanism mounted on top of the lower mechanism. In order to decrease inertial effects, and to improve back-drivability and transparency, the mechanism has only ground fixed actuators with cable drives (Ryu, et al. 2009).

Figure 2.16. Overview of a 6-DOF Haptic Device
(Source: Ryu, et al. 2009)

Another 6-DOF parallel haptic device can be seen in Figure 2.17. It is aimed to design a light weight system with ground fixed motors. (Lee, et al. 2001).

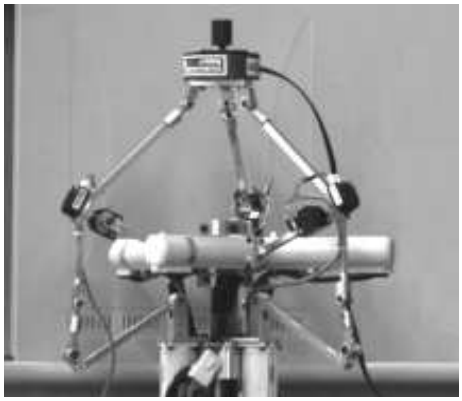

Figure 2.17. 6-DOF Parallel Haptic Device
(Source: Lee, et al. 2001)

The CAD representation a 6-DOF haptic device is designed by Gosselin et al can be seen in Figure 2.18. The device is a light-weight parallel-structure mechanism with the handle on its moving platform. It was designed for computer aided design or virtual sculpturing applications (Gosselin, et al. 2005)

Figure 2.18. CAD design of the haptic interface
(Source: Gosselin, et al. 2005)

Yoon et al. designed a 6-DOF haptic mechanism that was driven with servomotors as presented in Figure 2.19. In this work, the control of the system was also studied and a control method with gravity compensation and with force feedback by a force-torque sensor was employed to reduce the effects of unmodeled dynamics (Yoon and Ryu 2001).

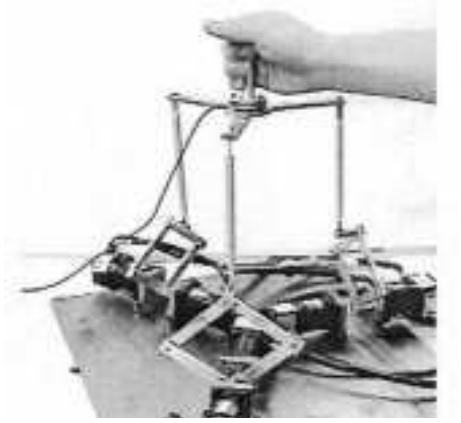

Figure 2.19. 6-DOF haptic mechanism
(Source: Yoon and Ryu 2001)

A CAD model of a spherical mechanism for a haptic system called “SHaDE” is shown in Figure 2.20. SHaDE was a 3-DOF haptic device that has a spherical geometry. Due the spherical geometry, the mechanism has only pure rotation around

all axes at its center point, where the handle of the joystick is located at. It is offered for high precision teleoperation and VR applications (Birglen, et al. 2002).

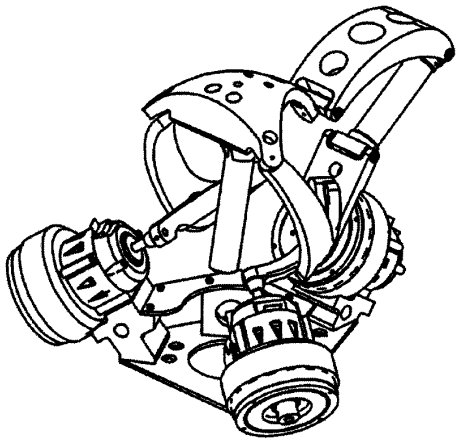

Figure 2.20. CAD model of SHaDE
(Source: Birglen, et al. 2002)

A general purpose 6-DOF haptic interface is presented in Figure 2.21. The structure is composed of a 6-DOF parallel base and a handle part. (Lee and Lee 2003)

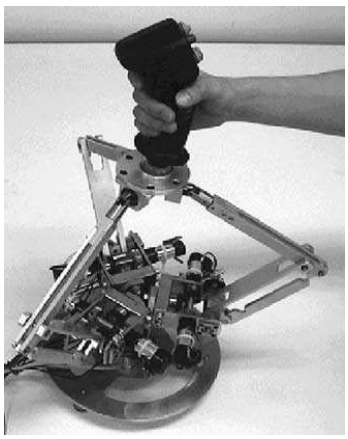

Figure 2.21. 6-DOF haptic interface
(Source: Lee and Lee 2003)

2.3.3. Hybrid Mechanisms

Hybrid manipulators have the advantages of a parallel structure and serial manipulators such as high loading capacity, manipulability, stiffness, high precision, robustness and relatively large workspace.

Commercial hybrid haptic devices are also available in the market for various types of applications such as Force Dimension's Delta based haptic devices. The Omega 6 haptic device (Figure 2.22) is a 6-DOF haptic device that has 3 active translations

3 passive rotations. It can apply 12 N continuous torque with resolution less than 0.01mm.

Figure 2.22. Omega 6 haptic device
(Source: Forcedimension 2010)

Another Delta based hybrid haptic device consists of 3-DOF Delta manipulator (Figure 2.23(a)) for translation motions and 2-DOF gimbal ball for the orientation motions (Figure 2.23(b)). (Uchiyama, et al. 2007).

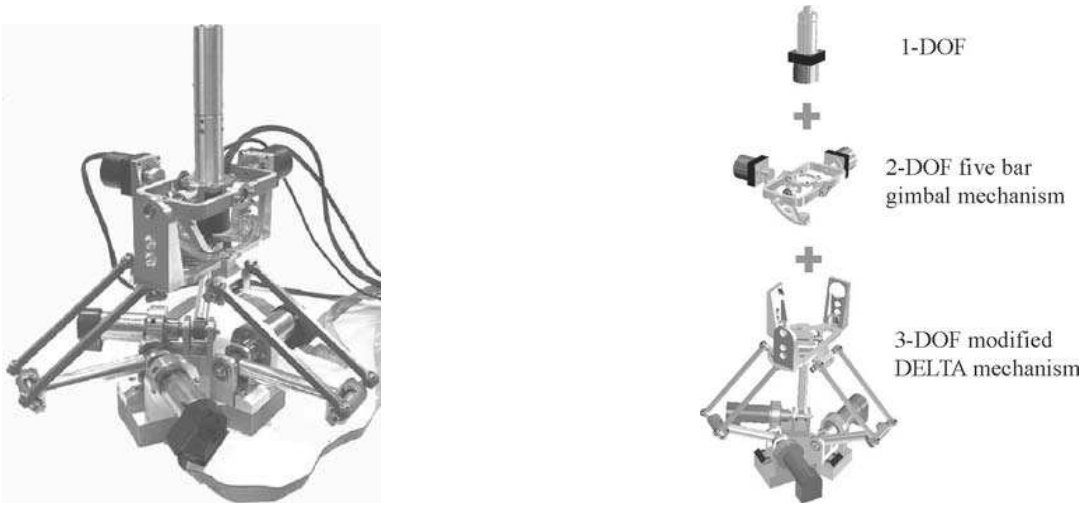

(a) (b)

Figure 2.23. 6-DOF mechanism: (a) Overview of the device, (b) DOF of the mechanism (Source: Uchiyama, et al. 2007)

2.4. Haptic Applications

Haptics technology is employed in various types of systems to accomplish important tasks ranging from portable robotic surgery tools to flight simulators. This section provides a review of haptic applications in two groups; (1) Teleoperation and (2) VR applications.

2.4.1. Haptics in Teleoperation

The concept of teleoperation can be briefly summarized as remote control of robotic systems. Although humans have the ability to manage many complex tasks, remote controlled robots is a requirement for some special tasks such as small scale manipulations, tasks that are take place in hazardous environments or remote control of a machine at a distant location.

Basically teleoperation systems are composed of a master and a slave subsystem. Currently, haptic devices find use in assistive surgical robotics and most of the teleoperation systems in which level of telepresence is required to be increased for improved tele-manipulability.

A haptic teleoperation with 5-DOF force feedback mechanism shown in Figure 2.24(a), and a 2-DOF microrobot shown in Figure 2.24(b) was proposed and experimentally tested. The disparity between the master and slave side of the system improves the controllability of the micro robot in the environment. (Vlachos and Papadopoulos 2008).

(a) (b)

Figure 2.24. Telemanipulation system: (a) Master haptic device, (b) Micro robotic platform (Source: Vlachos and Papadopoulos 2008)

All-terrain mobile robot, shown in Figure 2.25(a), is designed for haptic teleoperation applications. The mobile robot is equipped with various positioning systems such as sonar sensors, GPS module, wheel encoders, 3 axis gyro and accelerometer. PHANTOM Omni haptic device is the master mechanism of the teleoperation system. The master and slave systems were integrated with the communication equipments and control software as shown in Figure 2.25(b) (Horan et al. 2007).

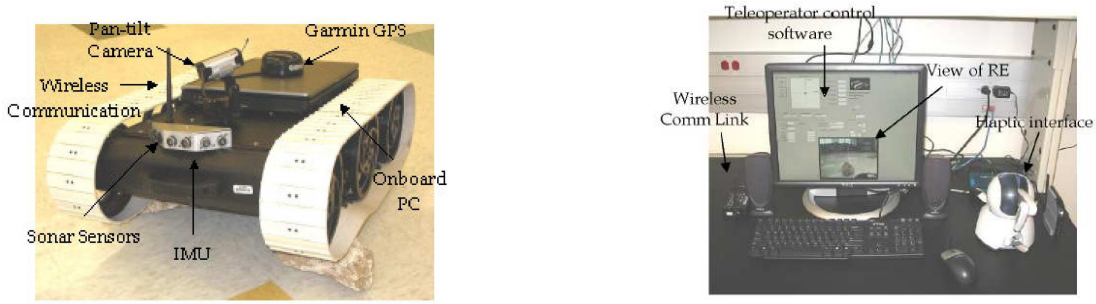

(a) (b)

Figure 2.25. Teleoperation system: (a) Prototype of a mobile robot, (b) Control Station (Source: Horan, et al. 2007)

A similar mobile robot designed for haptic teleoperation applications is shown in Figure 2.26. A mobile robot with multi sensory output is usually required to avoid obstacles in teleoperation applications. The sensory inputs are used to reproduce haptic force feedback to operator. Haptic feedback helps the operator to take the necessary actions to prevent the mobile robot from collisions (Lee, et al. 2005).

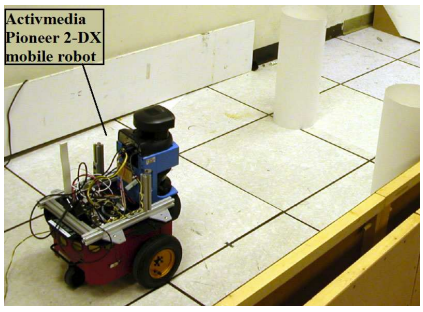

Figure 2.26. Teleoperation of a mobile robot (Source: Lee, et al. 2005)

A nanoscale tele-manipulation system has been developed with a commercial haptic device and atomic force microscope configuration (Figure 2.27). The researchers that configured this system suggest that haptics technology has the potential to provide intuitive, efficient and reliable way for quick manipulation of nano-scale manipulations. The master and slave side of the haptic teleoperation setup can be seen in Figures 2.27(a) and 2.27(b), respectively (Jobin, et al. 2005).

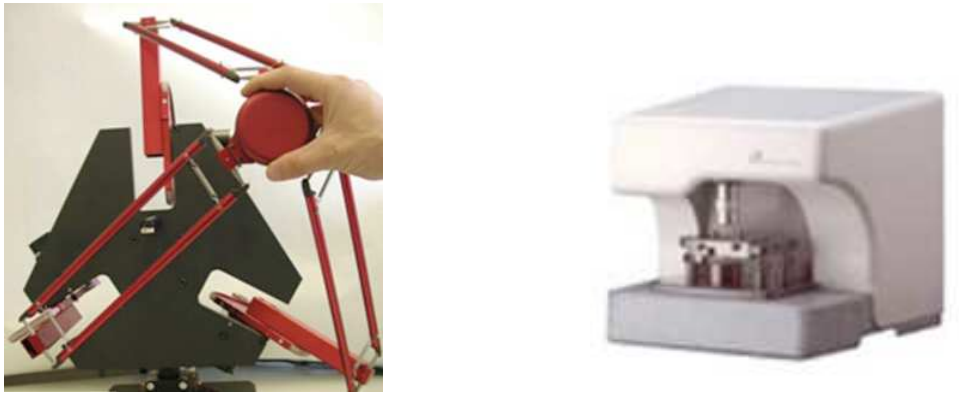

(a) (b)

Figure 2.27. Nano manipulation system: (a) Haptic device, (b) Atomic force microscope (Source: Jobin, et al. 2005)

Teleoperation of underwater construction machines is a typical example of hazardous environment operation. Haptics technology in teleoperation of underwater construction machines provides safer and more efficient underwater construction work.

An example for underwater haptic teleoperation application is shown in Figure 2.28. Camera systems usually do not provide good picture quality due to turbidity of the water. Hence, haptics technology along with the visual feedback provides a solution for this problem. (Hirabayashi, et al. 2006). Conventional manned underwater application and in developed haptic control system can be observed in Figures 2.28(a) and 2.28(b), respectively.

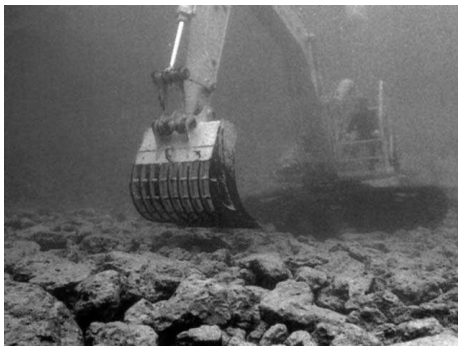

(a)

(b)

Figure 2.28. Teleoperation in hazardous environments: (a) Manned underwater backhoe, (b) Control room of developed system (Source: Hirabayashi, et al. 2006)

2.4.2. Haptics in Virtual Reality

Haptics technology increases the level of interaction between the user and the virtual environment in VR applications. Programmed virtual sensors provide sense of touch, which improves the quality of the virtual-presence. Other than the game industry, haptics in VR applications are used frequently in training and educational purposes such as medical simulators and especially for expensive and difficult trainings such as dental trainings.

A 6-DOF haptic device for dental surgery training system is presented in Figure 2.29. The designed haptic device is based on a modified 6-RSS parallel mechanism. It has ground fixed actuators that decrease the total inertia of the device. The kinematics of the device can be solved numerically. The singular configurations of the mechanism is identified and avoided for defined workspace (Cao, et al. 2007).

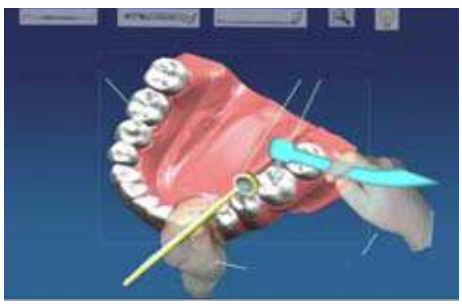

(a)

(b)

Figure 2.29. 6-DOF haptic device for dental training: (a) Virtual reality application, (b) CAD design of the mechanism (Source: Cao, et al. 2007)

Conventional design techniques with 2D mouse often require difficult design procedure. Virtual sculpturing and designing via haptic devices facilitates the procedure. A virtual sculpturing system utilizing with 6-DOF PHANTOM haptic device is shown in Figure 2.30. A haptics-based interface for this application is presented (Dachille, et al. 2001).

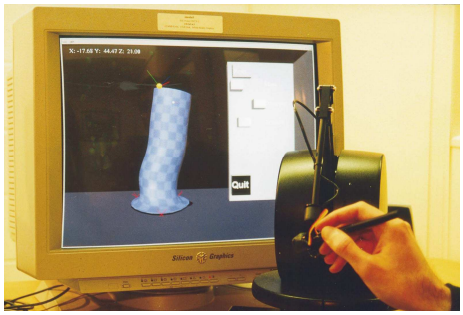

Figure 2.30. A virtual sculpturing system
(Source: Dachille, et al. 2001)

A virtual-reality surgical simulator for neurosurgeries is presented in Figure 2.31. The simulator reproduces effects of a surgical operation such as prodding, pulling and cutting (Wang, et al. 2006).

Figure 2.31. A virtual-reality surgical simulator
(Source: Wang, et al. 2006)

Haptics technology also offers solutions for very difficult tasks such as robot path planning. Haptic-aided robot path planning via a virtual robot facilitates the programming process. The user's interaction with the VR can define or modify critical

positions and collisions. An example for such an application can be observed in Figure 2.32 (He and Chen 2008).

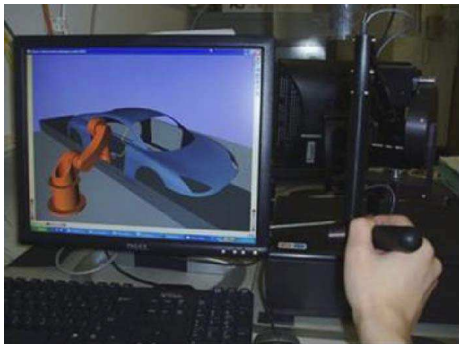

Figure 2.32. Robot path planning by virtual teleoperation
(Source: He and Chen 2008)

Following to the development of more affordable haptic mechanism, the haptic technology is applied in more specific applications such as rehabilitation systems. A haptic, patient monitoring system that is developed for monitoring the progress of the patient is presented by Ruba Kayyalil et al. The system is based on a haptic device (Figure 2.33) and VR applications that simulates simple exercises and monitors the performance of the user (Kayyalil, et al. 2008).

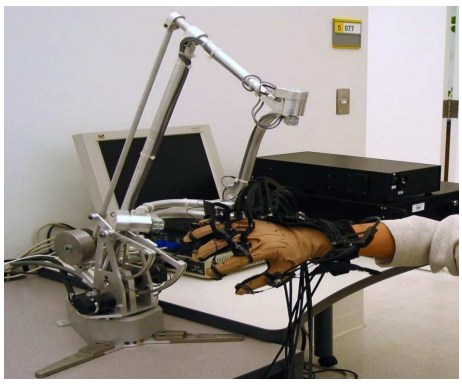

Figure 2.33. Haptic monitoring system in rehabilitation
(Source: Kayyalil, et al. 2008)

Moreover haptics are also used in haptic rehabilitation systems via applying force feedback in virtual-reality application. VR-based ankle rehabilitation system is presented by Rares F. Boian et al. Similar with the previous example the system

consists of a haptic mechanism (Figure 3.34) and a VR application that simulates control of virtual examples (Source: Boian, et al. 2003).

Figure 2.34. Haptic rehabilitation system
(Source: Boian, et al. 2003)

2.5. Conclusion

Today, various types of haptic systems are used in different types of applications. In order to identify these systems, previous systems are investigated and categorized by their; sensation types, kinematic structure and applications. Depending on the type of the mechanoreceptors, two types of sensation types in haptic systems are explained and related examples are presented. The kinematic structures of robot manipulators are listed and the advantages and disadvantages are discussed. For each type of kinematical structure, previously built haptic device examples are introduced. Finally, haptic applications are presented in two groups along with example systems.

In the next chapter, the components to configure the haptic devices are presented complying with the aim of the study.

CHAPTER 3

COMPONENTS OF A HAPTIC DEVICE

3.1. Introduction

Towards developing a new haptic desktop device, a designer has to identify the task that the haptic device will be employed. According to the environmental requirements, the design criteria of the haptic device have to be formed and the components should be selected. Although the components of a haptic device vary depending on the outlined types of the devices, basically all haptic systems are composed of mechanical, electro-mechanical, electronic and software parts. In this chapter, the commonly used components of the haptic devices are investigated and discussed.

3.1. Mechanical Components

Mechanical components of a haptic device can be listed as the mechanism, material and drive system. Mechanism selection is probably the most important phase in developing a haptic device. Therefore the selection procedure is outlined in the next chapter. In this section, only the materials and drive systems of the haptic devices are explained and discussed.

3.2.1. Materials

In haptic devices the specifications of the selected material for the mechanism are directly related with the quality of the haptic perception. The weight of the mechanical components must be minimized and the device has to have low inertia and high stiffness. Hence the most important specifications for the design haptic device material are;

i) Low density

ii) High strength and rigidity

In order to minimize the gravitational effects, haptic devices are manufactured from light weight materials such as aluminium, nickel, titanium alloys and plastics. Haptic devices transmit the forces that are applied by the user. Hence, the rigidity and the strength of the mechanism are important for precision and perception of the system. As a consequence strength to weight ratio is an important factor, which has to be considered in haptic device development.

Among the other alloys, aluminium alloys is the most remarkable material in haptic devices. In general aluminium alloys have reasonable price, good machinability, high corrosion resistance and vital specifications outlined above.

Non-metallic material plastics also provide good strength to weight ratio and very low cost which are used in many haptic devices. In mass production of the haptic devices, plastic injection moulding is an easy manufacturing process that is used for the manufacturing of the least important parts. Hence in general, the commercial haptic devices are composed of plastic and aluminium alloy parts and the custom haptic devices include only aluminium alloy components.

The two parallel haptic desktop devices from different companies are shown in Figure 3.1(a) and Figure 3.1(b). The Omega 3 is developed for more precise applications such as medical and micro manipulation applications therefore it has more rigid structure with polished aluminium kinematic links, joints and frame which can be seen in Figure 3.1(a). Falcon haptic device is particularly developed for the game industry. It has less precise joints and base manufactured from plastics, which can be seen in Figure 3.1(b).

(a) (b)

Figure 3.1. Parallel haptic devices: (a) Omega 3 from force dimension (Source: Forcedimension 2010), (b) Falcon from Novint (Source: Novint 2010)

Omni haptic device (Figure3.2) is the most cost-effective product of the Sensable Technologies and it has also a body that is a composed of aluminium and plastic materials.

Figure 3.2. Omni from sensible technologies
(Source: Sensable 2010)

3.2.2. Drive Systems

In haptics, drive systems are used for the transmission of the torques from actuators to the operator and the performance of the actuation system is more important with respect to the other robotic systems. Hence selection of the appropriate drive systems considering the type of the haptic device is important. The appropriate drive systems for a haptic device can be selected depending on the two broad classes

i) Admittance type devices
ii) Impedance type devices

Admittance haptic devices include force sensors that sense the applied force by the operator and adjust the operator's position according to the manipulated virtual or real object. Hence the traditional transmission mechanisms such as gears can be employed in admittance type haptic devices. Nevertheless, the precision loss due to the use of transmission mechanisms is an important fact, which has to be considered in haptic device design. Therefore, high efficient and precise gearing transmission technology such as harmonic drive is currently used in haptic devices. Harmonic drives provide nearly zero backlash, light weight and high torque reduction ratios. An example for an admittance type haptic interface is VISHARD7 which can be seen in Figure 3.3. VISHARD7 is a 6-DOF mobile haptic interface for large remote

environments. The haptic interface is built by using brushless DC motors coupled with harmonic drive gears that provide relatively high force feedback capacity (Peer and Buss 2008).

Figure 3.3. Mobile haptic interface VISHARD7
(Source: Peer and Buss 2008)

Previously presented haptic interface in Chapter 2, MGA haptic device is also a harmonic driven system with brushless DC motors and two force/torque sensors (Carignan, et al. 2009).

Figure 3.4. Force sensors of MGA exoskeleton haptic
(Source: Carignan, et al. 2009)

In contrast to the admittance haptic devices, in an impedance haptic device, position sensors sense the position of the operator, and then the computed forces are applied to the user. Therefore, impedance type haptic devices have to be back-drivable

which is possible with low inertial and low frictional drive systems. Today most of the commercially available haptic desktop devices such as Phantom, Omega and Falcon are impedance type haptic systems. They are back-drivable and have a common mechanical transmission system called Capstan drive mechanism (Figure 3.5). The capstan drive mechanism consists of tendon wrapped around pulley that actuates a semi-circular link. The ratio between the pulley's and the semi-circular link's diameters provides reduction that increases the force feedback capacity of the haptic systems. Capstan drive mechanism of a 1-DOF haptic paddle can be seen in Figure 3.5 (Bowen, et al. 2006).

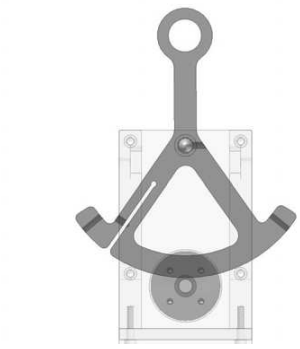

Figure 3.5. Capstan drive mechanism of a haptic paddle
(Source: Bowen, et al. 2006)

Capstan drive systems are also used in medical haptic devices. 5-DOF mechanism which has a more complex capstan system is presented in Figure 3.6 (Vlachos and Papadopoulos 2008).

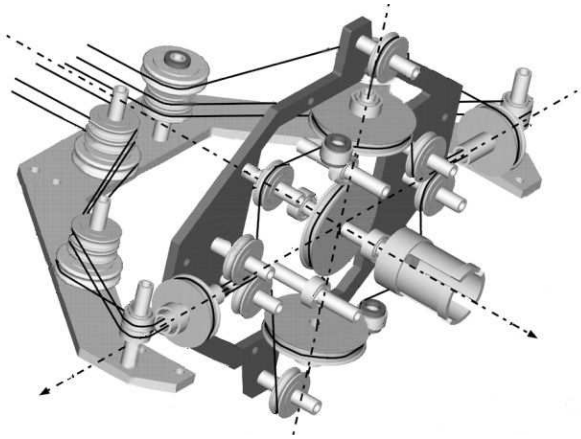

Figure 3.6. Capstan drive system of a medical haptic device
(Source: Vlachos and Papadopoulos 2008)

3.3. Electro-Mechanical Components

Electro-mechanical components of a haptic desktop device can be listed as the brakes, sensors and actuators. In haptics usually two types of sensors are used; position and force/torque sensors. Position sensors measure the angles or positions of the links and this sensory input is transmitted to the computers. Depending on the type of the haptic system, force/torque sensors are also used especially in admittance type haptic devices. Moreover brakes and motors are used for the actuation of the mechanism and the properties of the actuation system are directly related with performance of the haptic device. In this section, electro-mechanical components of a haptic device is presented and discussed.

3.3.1. Brake Systems

Haptic interfaces can also be categorized as active or passive interfaces depending on the employed actuators. Active haptic interfaces employ active motors, to provide active feedback to the user. On the other hand, passive haptic interfaces use dampers or brakes that dissipate the energy of the motion. In contrast to the active actuators, passive actuators such as brakes, dampers and clutches are actually stable components that they can only absorb the energy of the system. Therefore they can provide relatively larger forces without risking the user's safety. Furthermore it can improve the stability of the system. However passive actuators can only simulate some models such as high stiff wall or any rigid surface but they cannot simulate a model of an elastic surface or moving object. Nevertheless, due to the outlined advantages, dissipative components are recently employed in some haptic devices for better force-feedback capabilities and higher perception levels. Currently mechanic friction, electro-magnetic, magneto-rheological, electro-rheological brake systems are employed and tested in haptic devices.

Mechanical brake system of the previously presented, 4-DOF wearable passive haptic interface’s is shown in Figure 3.7. The brake system of the device is located at the top of the exoskeleton and the mechanism consists of separate transmission cables for actuation with brake mechanism. In this example, the requirements of an

exoskeleton haptic device such as simplicity, lightweight, high safety and hard-contact simulation are provided by passive actuation (Lelieveld and Maena 2006).

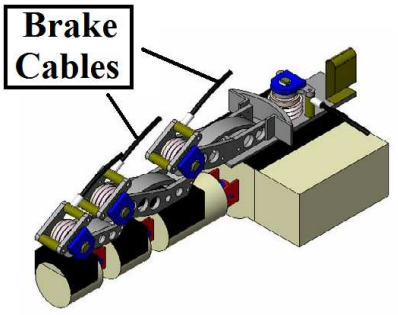

Figure 3.7. Wearable passive haptic interface
(Source: Lelieveld and Maena 2006)

Zitzewitz et al. Presented a hybrid actuation concept with motor, spring and electro-mechanically actuated disc brake. The brake system is selected considering the 5Hz bandwidth requirements which can be seen in Figure 3.8 (Zitzewitz, et al. 2008).

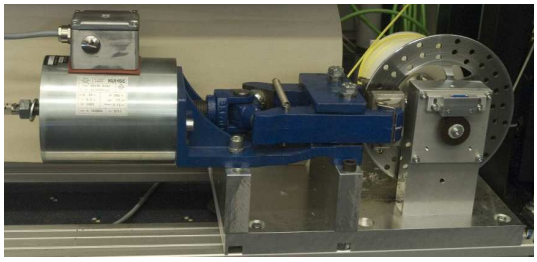

Figure 3.8. Disk brake system for a haptic device
(Source: Zitzewitz, et al. 2008)

Another example for hybrid actuation is the 2-DOF haptic interface that is used for medical purposes is shown in Figure 3.9. The device has rotational and translational axes actuated by both active and passive actuators. The combination of active motors and passive brakes improves sensation levels by reflecting the natural friction and high level force feedback of the haptic colonoscopy (Samur, et al. 2008).

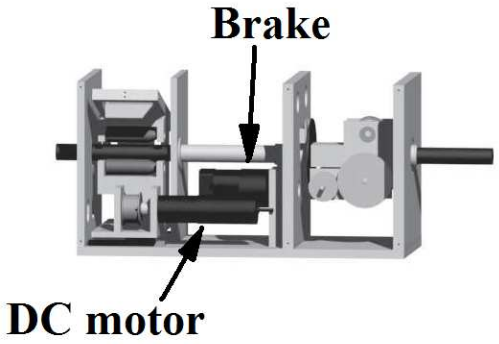

Figure 3.9. Hybrid device with mechanic brake and motors
(Source: Samur, et al. 2008)

Electromagnetic brakes such as eddy current brakes (ECB) are also employed in haptic systems. Some of the specifications of the ECBs such as programmable damping rates, applicability to the linear motion, high frequency responses make them very appropriate for passive haptic interfaces. The development and implementation of an ECB to a haptic interface is proposed by H. Andrew et al. 2-DOF mechanism and the components of the device can be seen in Figure 3.10 (Andrew, et al. 2008).

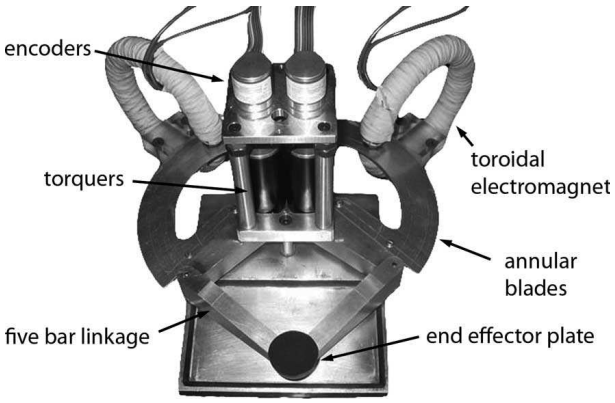

Figure 3.10. Hybrid device with ECB's
(Source: Andrew, et al. 2008)

Magneto-rheological (MR) fluids and electro-rheological (ER) fluids are types of smart materials. They are both capable to change their viscosity reversibly within milliseconds by controlling the applied magnetic or electric field. This feature can be applied to wide range of applications such as variable damping systems. Especially in haptics due to the short response time and damping abilities of both MR and ER fluids are used as braking systems. An example of MR fluid brake system in haptic devices is

presented by W.H. Li et al. The mechanism (Figure 3.11) is a conventional 2-DOF Gimbal mechanism, employed with two MR actuators (Li, et al. 2007).

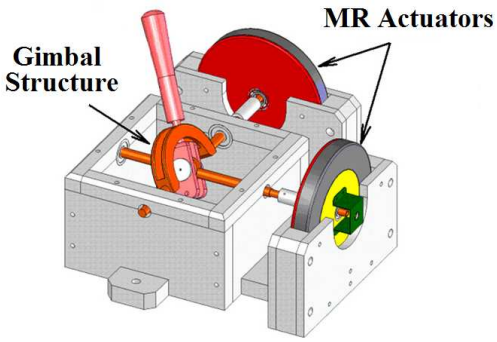

Figure 3.11. CAD representation of mechanism
(Source: Li, et al. 2007)

A 2-DOF haptic system with ER actuators is presented by Takehito Kikuchi et al. for rehabilitation purposes. In order to guarantee the safety of the user, the system is configured with only electrically controllable brake that is shown in Figure 3.12 (Kikuchi, et al. 2007).

Figure 3.12. ER Brake
(Source: Kikuchi, et al. 2007)

3.3.2. Motors

Motors are the active actuation components in haptic devices. The performance of an active haptic device is directly related with the characteristics of the actuators. In order to provide high level sensations in a haptic interface, the actuators of the system must have low inertia, low friction, low torque ripple, high back-driveability, low backlash and high torque ratings. The selection of the appropriate actuators to meet the requirements of the haptic device is important. Currently various types of active actuators are employed in haptic desktop devices such as pneumatic, hydraulic, shape memory alloys (SMA), piezoelectric, pneumatic muscle, ultrasonic, magnetic and electrostatic actuators.

Currently, DC motors are the most common actuation systems utilized in haptic devices. Most of the haptic devices in literature, including the commercial ones are configured with DC motors. DC motors are the pioneer electrical actuation method with respect to the other actuation methods. The performance, limitations, dynamics and control methods of the DC motors are well known. Moreover, DC motors have low cost, high reliability, and simple structure. Hence in robotics, actuation with brushed or brushless DC motors is the most preferred method. However, in haptic devices other actuation systems can provide better results.

Shape memory alloys (SMA) are smart materials that have the ability to change its dimension via heat variations. Recently SMAs are employed in various types of applications including haptics. Although it seems that the SMA actuators are only employed in tactile haptic devices, SMA actuators have the potential to be used in SMA actuated haptic devices. Schematic representation of an 8x8 pin array haptic tactile display system is shown in Figure 3.13 (Jairakrean and Chanthasopeephan 2009).

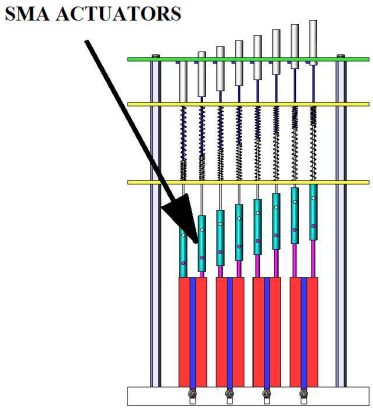

Figure 3.13. SMA actuators for tactile display
(Source: Jairakrean and Chanthasopeephan 2009)

Pneumatics (Figure 3.14(a)) converts air pressure to rotational or linear motion. The main advantage of the pneumatic actuation is the flexibility of the actuators which is necessary in a device that interacts with human. Due to the difficulties of position and force control, the pneumatics is not common in haptic devices. An example for pneumatic parallel haptic interface is proposed by Masahiro Takaiwa et al. The proposed device is a parallel mechanism that includes 6 pneumatic actuators and potentiometers as shown in Figure 3.14(b) (Takaiwa and Noritsugu 1999).

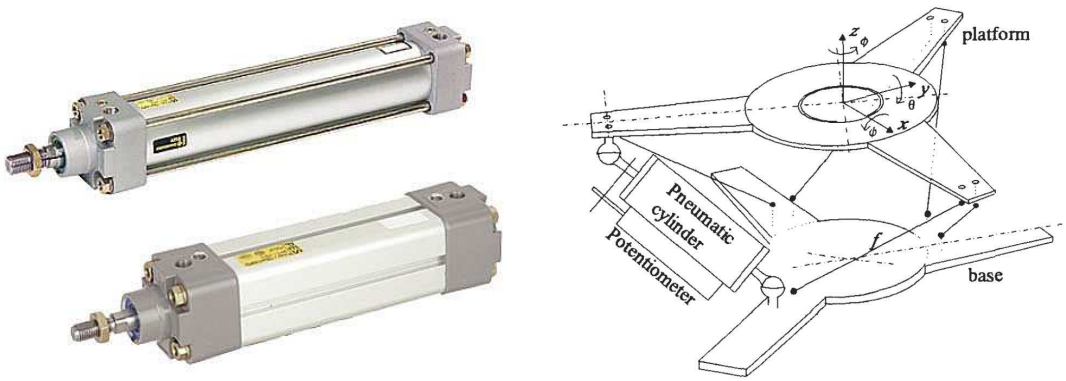

(a) (b)

Figure 3.14. Pneumatics in haptics (a) Pneumatic actuators (Source: Directindustry 2010), (b) Parallel haptic device (Source: Takaiwa and Noritsugu 1999)

Similar to the human muscles, pneumatic muscle actuators (PMA) are contractile components work with pressurized liquid or gas. The specifications of the PMAs are similar to the conventional pneumatic actuators, but the power/weight ratios

of the PMAs are relatively greater. Due to the presented advantage, PMA actuators are suitable for exoskeleton haptic devices. A 7-DOF PMA actuated exoskeleton haptic device is presented by N.Tsagarakis et al. (Tsagarakis, et al. 1999).

Figure 3.15. PMA actuators
(Source: Salonix 2010)

Ultrasonic motors are piezoelectric motors that are actuated by ultrasonic vibrations. Similar to the DC motors, they consist of a rotor and a stator which is produced by piezoelectric materials. The ultrasonic motors are driven by two sinusoidal signals with a different phase. Associated with the phases of the signals the ultrasonic actuator has three phases; free, active and fixed phase. Thus ultrasonic sensors are capable to actuate a haptic device as a hybrid (passive/active) system without using brakes or clutches. Conceptual design of a wearable exoskeleton haptic for the index and thumb fingers can be seen in Figure 3.16. The entire mechanism is actuated with only four ultrasonic actuators that reflect bi- directional forces. (Choi and Choi 1999).

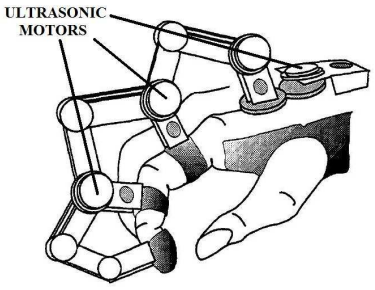

Figure 3.16. Exoskeleton haptic with ultrasonic actuators
(Source: Choi and Choi 1999)

Magnetic levitation actuators are probably the most interesting ones among the other actuators. The theory is based on suspending a handle object in magnetic field. A study on developing a magnetic haptic device is presented by Berkelman et al. 6-DOF device has motion ranges of ±5 mm and ±3.5 degrees in all directions and can generate 20N force, 1.7 Nm torque (Berkelman, et al. 1995). A commercial magnetic levitation haptic is the product of Butterfly Haptic Inc. which can be seen in Figure3.17.

Figure 3.17. Magnetic levitation haptic interface
(Source: Butterflyhaptics 2010)

Another method of actuation method in haptic devices is the electrostatic actuation. A 2-DOF linear haptic device with two electrostatic actuators is presented in Figure 3.18. This device is designed for neuroscience applications and non-magnetic actuators are employed in the system (Hara, et al. 2009).

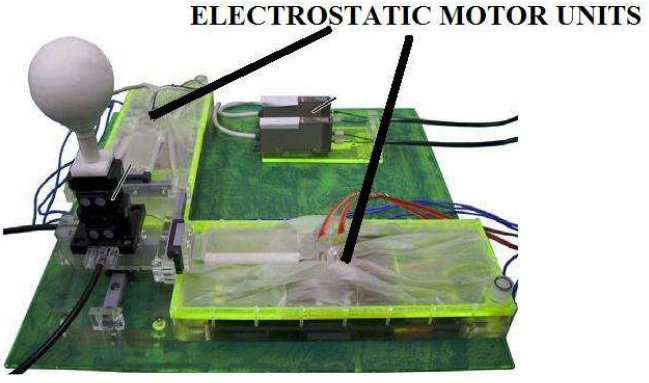

Figure 3.18. Haptic joystick with Electrostatic actuators
(Source: Hara, et al. 2009)

3.3.3. Sensors

In haptic device design, appropriate sensor selection is important for the electro-mechanical precision of the mechanism. Essential sensors of a haptic device are force/torque and position sensors. Position sensors can be categorized in two groups; analog and digital sensors. In general, hall-effect and resistive sensors are frequently employed in haptic devices due to their high resolution and low cost. However the noisy nature of the analog signals needs extra care during transfer and conversation to the digital signals. Besides potentiometers have various technical specifications that have to be evaluated carefully for use in haptic devices, such as mechanical resolution, linearity errors and resistance tolerance. On the other hand, digital encoders provide more accurate and noise free signal therefore digital encoders are more convenient for haptic applications. Nevertheless today, the cost of the digital encoders is relatively high and supplied resolution is limited.

Currently commercially available haptic devices include both optical encoders and potentiometers. 6-DOF PHANTOM haptic device includes optical encoders and potentiometers on its active and passive joints respectively.

An example for the use of potentiometers is shown in Figure 3.19. Previously presented 2-DOF gimbal mechanism has two potentiometers for each of the axes (Park, et al. 2004).

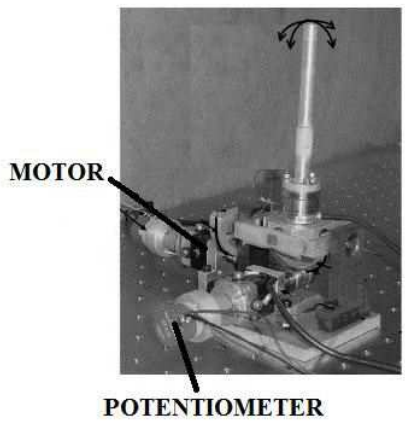

Figure 3.19. Sensors of a 2-DOF haptic joystick
(Source: Park, et al. 2004)

CAD representation of a 1-DOF haptic interface for rehabilitation applications can be seen in Figure 3.20. The mechanism consists of an optical encoder and a force sensor (Khanicheh et al. 2008).

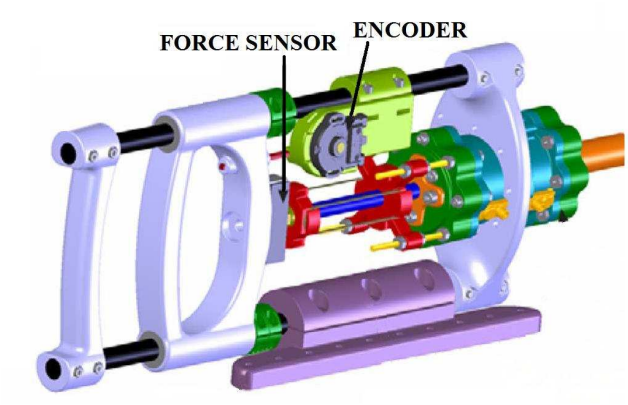

Figure 3.20. Force sensor and encoder of a haptic interface
(Source: Khanicheh, et al. 2008)

A variety of sensors are designed to measure forces/torques for different applications. The components of a force/torque sensor can be categorized in two groups as; the construction of the sensor and the sensing element. The construction of force sensors has to be designed considering the requirements of the application and the sensing element. Currently, strain gauges and piezoresistive sensing elements are the most common sensing elements in the force/torque sensor design. In admittance type haptic devices, both custom and commercial (Figure 3.21) type force/torque sensors can be used. Although the commercial type sensors have relatively high cost, they can provide more accurate and reliable measurements.

Figure 3.21. Load cell
(Source: Honeywell 2010)

3.4. Electronic Components

Data acquisition (DAQ) cards and motor amplifiers can be listed as electronic components of a haptic device. DAQ cards are the systems that measure, process, convert and transmit real world data to computers. Although the components of a DAQ system vary, depending on the specified tasks, DAQ systems may include, analog to digital converters (ADC), digital to analog converters (DAC), encoder decoders, counters, timers, digital inputs and outputs. In this section, appropriate DAQ systems for a haptic device are investigated. Commercially available DAQ systems are reviewed and previously built custom DAQ designs for haptic device are presented.

3.4.1. Commercial Data Acquisition Systems

During the development of a robotic system, commercial DAQ systems provide fast and reliable environment for initial tests of the integrated mechanism. Various DAQ cards are available for haptic device development with varying low prices. The primary specification of a DAQ system in haptic device design is the sampling rate requirement of the system. The selected commercial DAQ acquisition system has to support at least 1 KHz sampling rate (Tanner and Niemeyer 2006). Moreover the supported software environments such as Simulink and LabVIEW are also important for easy programming phases and initial test of the device.

Some of the commercial DAQ system providers can be listed as National Instruments (NI), Labjack, Quanser, Sensoray, Diamond Systems, dSpace, IOTech, Servo2go. NI is a hardware and software developer that provides various types of DAQ systems for different types of applications. An example for the product of National Instruments is NI PCI-6035E DAQ card, that supports 200kHz sampling rates and has 16-bit twenty-four analog inputs, 12-bit two analog outputs, eight bi-directional digital channels and 24 bit counter and timers (Figure 3.22). The system is fully compatible with Labview Software development environment.

Figure 3.22. NI PCI-6035E
(Source: NI 2010)

Labjack provides low cost DAQ solution for robotic applications. Labjack U3 DAQ system (Figure 3.23) provides 2.5 to 50 kHz sampling rates. It has 12-bit, sixteen analog inputs, 10-bit two analog outputs, and sixteen flexible digital channels and it provides LabVIEW communication library via USB port.

Figure 3.23. LABJACK U3
(Source: Labjack 2010)

High performance Quanser Q8 Hardware in the Loop (HIL) board (Figure 3.24) from Quanser Consulting Inc. has eight 12-bit D/A converters, eight 14-bit A/D converters, eight quadrature encoder inputs and thirty-two digital I/O channels. The card provides approximately 56 kHz sampling rate and real time applications. The device supports both LabVIEW and Matlab Simulink programming languages.

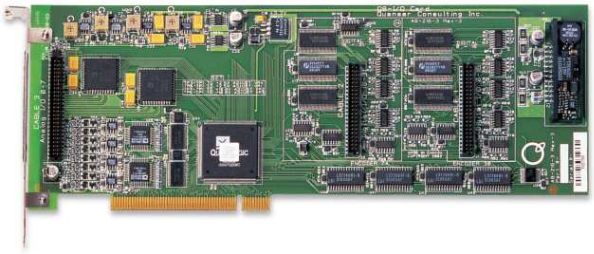

Figure 3.24. QUANSER Q8 hardware in the loop control board
(Source: Quanser 2010)

3.4.2. Custom Data Acquisition Systems

Towards developing an end product, custom designed and manufactured data acquisition cards and drives for the developed system are a necessity. Therefore, in this thesis study, it is intended to design customary data acquisition system for haptic mechanism. Thus, previously developed custom DAQ systems are reviewed and essential technologies are investigated.

As a result of the literature survey, it is oserved that PIC© (Programmable Interface Controller) based DAQ cards via serial port (RS-232) is commonly used in most haptic device designs. PIC is a popular microcontroller that is developed by Microchip Technology Inc. It is used in many digital control applications due to their low cost, easy development process, wide availability and high ability.

A haptic glove for color detection system is shown in Figure 3.25. The system occupies color sensors and tactile display to sense the color information and to reflect the user. The custom DAQ card of this system is based on a dsPIC30F4011 digital signal processor that communicates via RS-232 communication port (Schwerdt, et al. 2009).

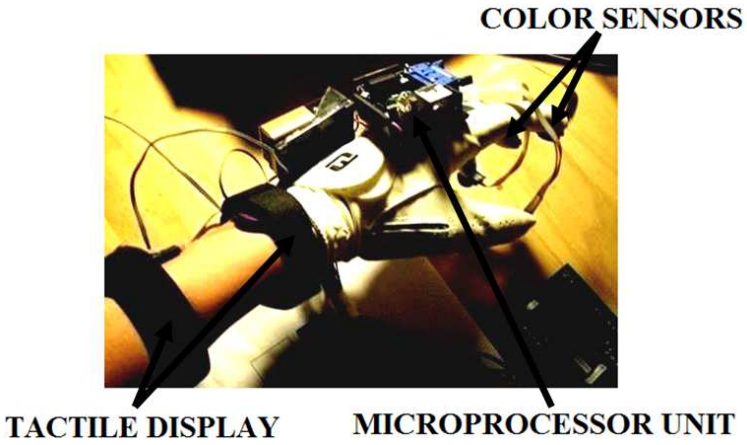

Figure 3.25. Tactile display haptic with color sensors
(Source: Schwerdt, et al. 2009)

Another tactile haptic study is presented by Pierre Payeur et al. The study focuses on development of a tactile sensory module with force sensitive transducers. The DAQ card (Figure 3.25) of the device is also configured with a PIC microprocessor via RS-232 which operates at 19200 baud rate (Payeur, et al. 2005).

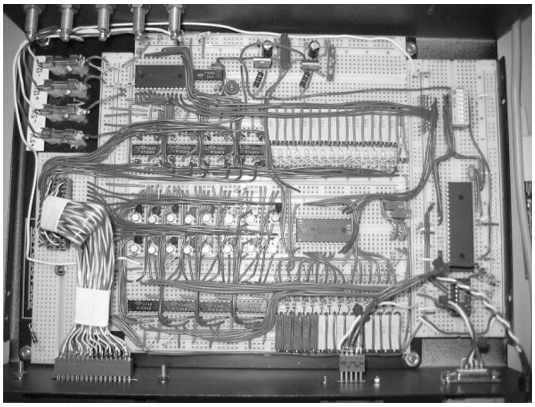

Figure 3.26. DAQ system of the sensor array
(Source: Payeur, et al. 2005)

3.5. Computer Control and Virtual Reality Software

Computer controller and VR application is required for the initial tests of a haptic system development. Hence appropriate computer controller and VR development softwares are investigated. Similar to the general robotic applications, high level programming languages such as Matlab (Simulink) and LabVIEW can be

used for the performance tests of the developed haptic devices. Both programming languages have the capability to develop real time applications and also include VR tools. Following to the initial test, respectively lower level software development languages are used in order to create final computer controller software, similar to the commercial haptic interfaces. In this section, possible haptic controller developer environments, LabVIEW and Matlab Simulink, are presented with examples.

3.5.1. Simulink

Simulink is graphical programming environment developed by MathWorks. It provides modelling, simulation and analyse tools for mechanical, electronic and electro-mechanical systems. Programs are developed using graphical programming blocks and a programmable set of block libraries. Simulink is widely used in control theory and digital signal processing for both frequency and time domain simulations. It supports two real-time working environments as Windows Real-Time target and xPC Target both compile the simulink code for HIL tests.

A mobile haptic device called VIDET can be seen in Figure 3.26 it is designed for visually impaired users. 3-DOF wire tension control system of the device is developed via simulink (Smid and Melchiorri 1998).

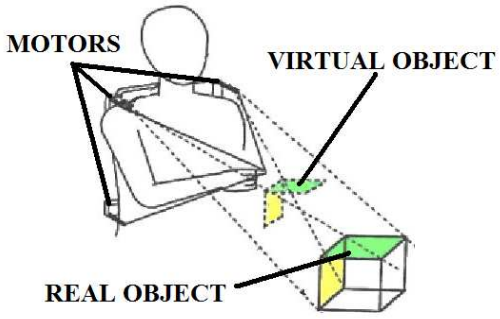

Figure 3.26. 3-DOF mobile haptic device
(Source: Lar.deis 2010)

3.5.2. Labview

LabVIEW is a product of National Instruments, which is also a graphical programming platform. It is commonly used by researchers and engineers for data acquisition, instrument control, data analysis, embedded system design and automation purposes. It also provides time domain applications and VR tools.

An example for VR application with LabVIEW is presented in previously shown 2-DOF joystick. The created 3D application for the test of the system can be seen Figure 3.27 (Li, et al. 2007).

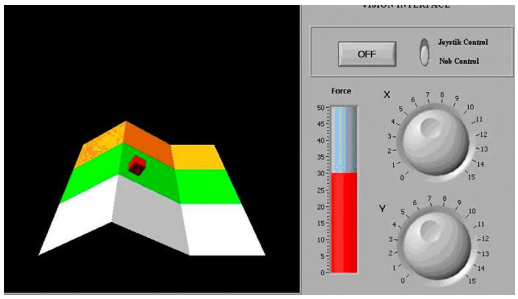

Figure 3.27. 2-DOF mobile haptic device
(Source: Li, et al. 2007)

3.6. Conclusion

In this chapter, necessary components of a haptic desktop device are investigated and appropriate components are compared. The material specifications for haptic devices are listed and common materials are presented. Two types of haptic systems are introduced. Considering the types of the haptic system, appropriate drive systems are explained. The importance of the actuation system for the performance of the device is addressed. For each component of the actuation system appropriate motors, brakes and drive mechanism are investigated. Both the custom and the commercial data acquisition systems for the developed mechanisms are reviewed and their specifications are presented. Finally, software development languages for the initial test of the system are given along with their examples.

In the next chapter mechanism selection, design phases and the kinematic parameter determination process of are explained.

CHAPTER 4

MECHANISM DESIGN

4.1. Introduction

During the development process, from the idea to tangible product, all design processes consist of different phases. Identification of design phases provides fast and reliable design process. The process of design that is used for the development of the mechanism is represented schematically in Figure 4.1.

The design of the mechanism begins with the identification of task. Evaluating the design parameters, the conceptual designs are formed and final design of the prototype mechanism is configured via simulations.

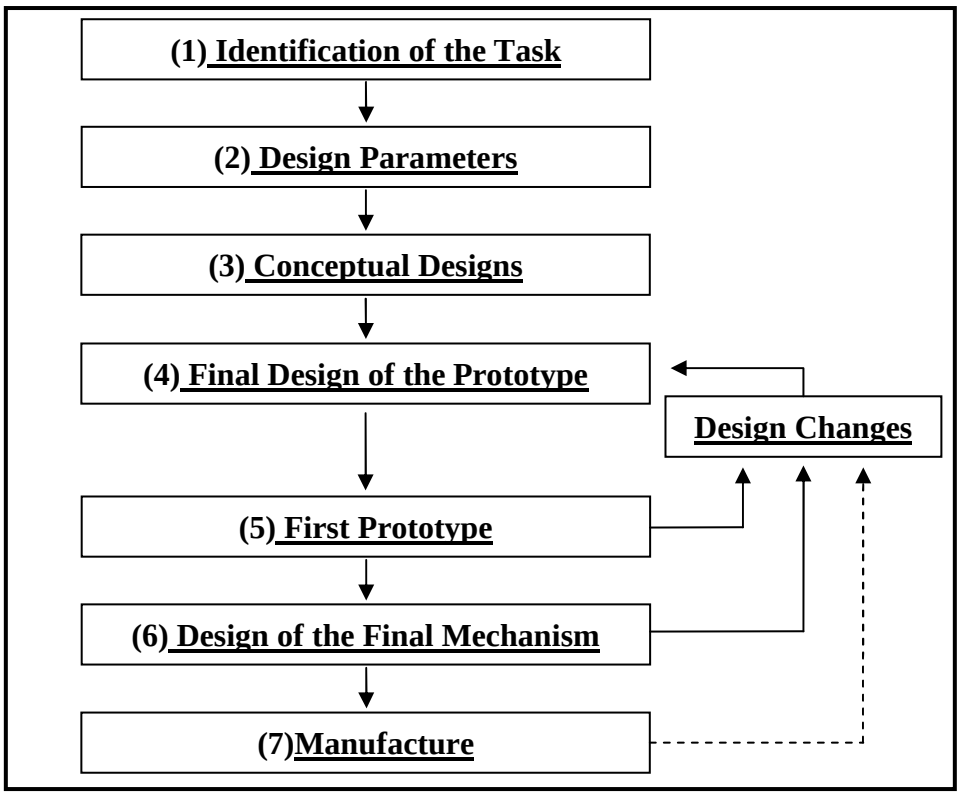

Figure 4.1. General design phases

The design of the prototype mechanism is manufactured and validation tasks are conducted. Complying with the test results, necessary design changes are identified and the design of the prototype mechanism is reconfigured. Finally, the necessary design changes are applied, the final design is simulated and the optimal design configuration is manufactured.

This chapter describes the study towards design and analysis of a novel 6-DOF hybrid haptic device that is composed of R-CUBE based active 3-DOF translational motion and passive 3-DOF orientation mechanism for rotational motion monitoring. The design procedure of the mechanism is explained in the order of the general design phases as outlined in Figure 4.1. The evolution of the system is shown with figures and geometric design procedure is explained. Finally the kinematic and force analysis formulas that will be used for position and torque control of the system are presented and explained.

4.2. Identification of the Task and Design Criteria

This thesis outlines the design of a general purpose haptic device for fine VR and teleoperation applications that require higher level of precision. In order to develop a general purpose haptic device a kinaesthetic desktop device is selected since it supports a wide variety of applications. The hybrid mechanisms have both the advantages of serial and parallel structures as discussed in Chapter 2. Therefore, the structure of the mechanism is selected to be configured as a hybrid structure.

Table 4.1. Design criteria of the haptic device

Sensation	Kinaesthetic
Structure	Hybrid
Concept of Structure	Desktop Device
Footprint	<150-200 mm^2
DOF	≥6
Force feedback	Translation $\vec{u}_1$, $\vec{u}_2$, $\vec{u}_3$
Workspace	>100 W x 100 H x 100 D mm
Continuous exertable force	> 0.8 N
Nominal Resolution	< 0.1 mm

The device is designated to provide feedback signals to determine the pose of the rigid body in space, therefore it should be configured as a 6-DOF mechanism. Only point type contact is considered for this thesis, so the DOF can be grouped as 3-DOF active translational and 3-DOF passive rotation. Considering the task requirements the design criteria of the mechanism are listed in Table 4.1. The workspace, continuous exertable force and the resolution of the system are selected to be compatible with the commercial haptic desktop devices that are reviewed in Chapter 2.

4.3. Conceptual Designs

According to the specified design criteria, the possible mechanism types for the hybrid structure reviewed in two groups, translation and orientation mechanisms. For translational mechanism, Delta, Cartesian Parallel, and R-Cube manipulators are considered and for orientation mechanism Agile Eye, Hybrid-Spherical and Serial-Spherical manipulators are considered in conceptual designs (Dede, et al. 2009).

4.3.1. Translation Mechanisms

Delta robot (Figure 4.2) is a 3-DOF parallel manipulator with 3RRNR structure that is used for translational motions for various haptic device designs. It has seventeen links connected with twenty-one joints that are actuated by three ground fixed rotary motors. It has coupled motion and its structure provides high resolution, manipulability and high loading capacity with relatively limited workspace.

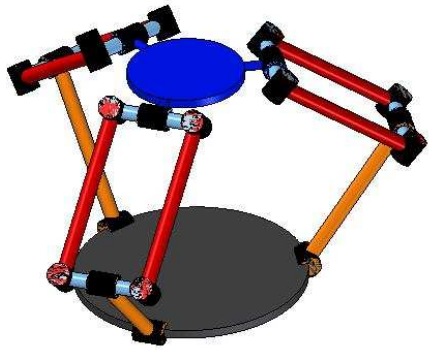

Figure 4.2. Delta manipulator

Cartesian manipulator is a 3-DOF parallel manipulator with 3PRRR structure. It can generate only translational motions (Figure 4.3). It has three legs that consists eleven links connected with twelve joints including base and platform. The actuation is provided by three prismatic joints with linear actuators. The motion of the manipulator is de-coupled in the direction of the prismatic axes.

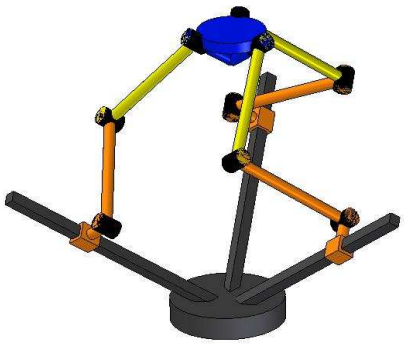

Figure 4.3. Cartesian manipulator

R-CUBE manipulator is a 3-DOF parallel manipulator with 3NRRR structure (Figure 4.4). It can generate translational motions with only revolute joints. It has three legs and seventeen links connected with twenty-one revolute joints. The motion of the moving platform is directly related with the input of the first links, therefore the structure has decoupled motion making use of rotary actuators. Its kinematic analysis is simple with respect to other manipulators due to the de-coupled motion. The singularities of the manipulator only exist at the limits of the workspace which is easy to avoid (Li et al. 2009).

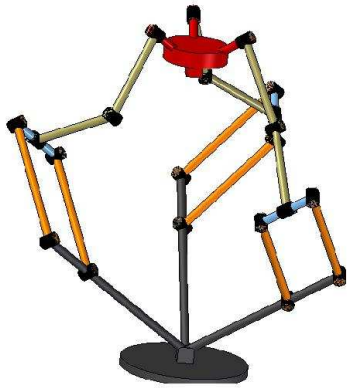

Figure 4.4. R-CUBE manipulator

4.3.2. Orientation Mechanisms

Agile Eye is a 3-DOF parallel manipulator with 3RRR structure (Figure 4.5). Its workspace is a 140° cone with ±30° in torsion. It has eight links connected with nine joints. As a constructional advantage, it has ground fixed sensors. The structure has coupled motion.

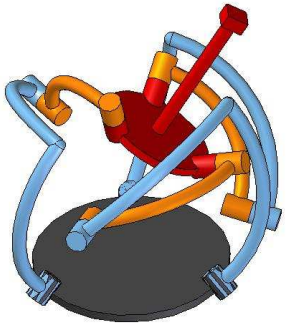

Figure 4.5. Agile eye

Hybrid-Spherical is a 3-DOF hybrid manipulator with 2RE+R structure (Figure 4.6). Its workspace is a spherical surface with ±90° (x) ±90°(y) ±120°(z). It has four links connected with six joints. It has 2 ground fixed and 1 moving sensors.

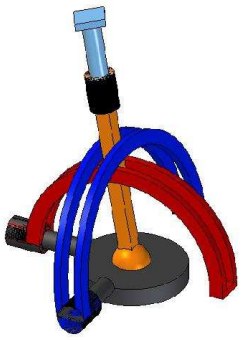

Figure 4.6. Hybrid-spherical manipulator

Serial Spherical Manipulator is a 3-DOF serial manipulator with RRR structure (Figure 4.7). As a consequence of its serial structure, it has large workspace with a range about ±120° around all directions, but it has two moving sensors.

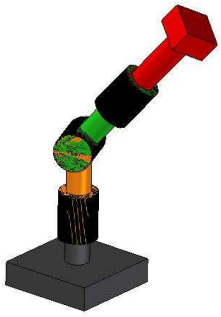

Figure 4.7. Serial-spherical manipulator

Table 4.2. Comparison of translation mechanisms

Mechanism	Delta	Cartesian	R-CUBE
Number of Joints	21	12	24
Number of Links	17	11	17
Kinematic analysis	Complex	Simple	Simple
De-coupled motion	No	Yes	Yes
Actuation	Revolute	Prismatic	Revolute
Ground fixed motors	Yes	Yes	Yes
Types of joints	R	R-P	R

The comparison table of the conceptual designs for translation and orientation mechanisms are shown in Tables 4.2. and 4.3, respectively. These two tables are used to select the configuration for the prototype of the hybrid mechanism.

Table 4.3. Comparison of the orientation mechanisms

Mechanism	**Agile eye**	**Hybrid - Spherical**	**Serial-Spherical**
Number of Joints	9	6	3
Number of Links	8	4	4
Kinematic analysis	Easy	Partially Complex	Complex
De-coupled motion	No	Yes	No
Workspace	Cone 140° with ±30° torsion	±90° ±90° ±120°	±120° ±120° ±120°
Sensation	Revolute	Revolute	Revolute
Ground fixed sensors	Yes	Partially	No
Types of joints	R	R-S-Sl	R

4.4. The First Prototype Mechanism

Considering the specifications of the conceptual designs outlined above, R-CUBE structure has unique properties as a haptic device mechanism. The structure of the mechanism includes only revolute joints, which increases the manufacturability and decreases the cost. The decoupled motion results in straight forward direct kinematics solution and static force analysis of the system. In haptics, due to the random motion of the operator, one of the most important facts is the singularity positions. Singularity analysis of the system is discussed (Li et al. 2009) and R-CUBE is proven to allow prevention of singularities with a proper design. Therefore, among the other translation mechanism candidates, R-CUBE mechanism is selected. Hybrid-Spherical manipulator consists of revolute, spherical and sliding joints at once and it has also difficult manufacturing and assembling processes because of its complex structure. Nevertheless, this structure is a conventional mechanism for many control applications including game consoles. Hence, as a tentative mechanism hybrid-spherical manipulator structure is demounted from joystick and employed into the system.

The entire system is manufactured from stainless steel due to its resistance to corrosion and heavy loads with laser cutting technology. Laser cutting technology provides high precision and reduced contamination for the links. Sliding joints are selected for their low cost and assembly easiness, even though it decreases the precision. Stepper motors are used as the actuators because of their low cost. Manufactured prototype system with orientation and translation mechanisms can be observed, in Figure 4.8 with 1 and 2, respectively.

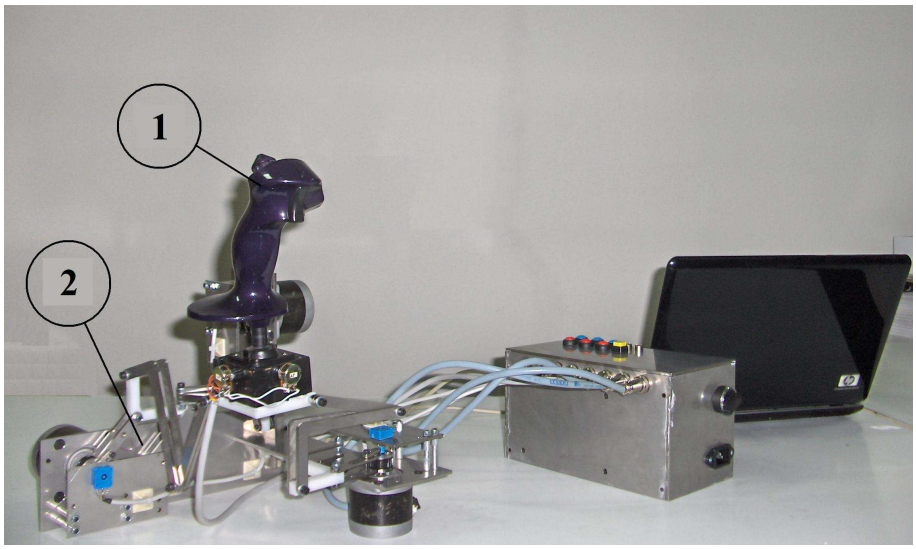

Figure 4.8. Manufactured prototype mechanism

The manufactured mechanism is integrated with other components of the system and tested. Although the prototype system cannot be employed as a haptic system, the initial tests of the prototype system provide promising results for its manipulability.

4.5. Design of the Final Translation Mechanism

Design of the translational mechanism is presented into three sections (1) Structural design parameters, (2) Mechanical part designs and (3) Link parameter determination. In the first subsection, the design criteria of the mechanism are identified. The necessary mechanical component designs are developed in the second subsection and finally, in the third subsection the dimensions of the links are determined.

4.5.1. Structural Design Criteria

In the prototype mechanism, the original structure of R-CUBE had some actuation problems due to the unequally distributed gravitational effects. Hence, the original structure of R-CUBE is reoriented and the effect of gravity is distributed

equally to all actuators. Apart from that, such an oriented configuration also facilitates the controller design and gravity cancellation algorithms.

The original structure configuration and the proposed configuration are shown respectively in Figures 4.9(a) and 4.9(b). The rotation of the structure is based on isometric projection problem, which is explained in the following section (Carlbom and Paciorek 1978).

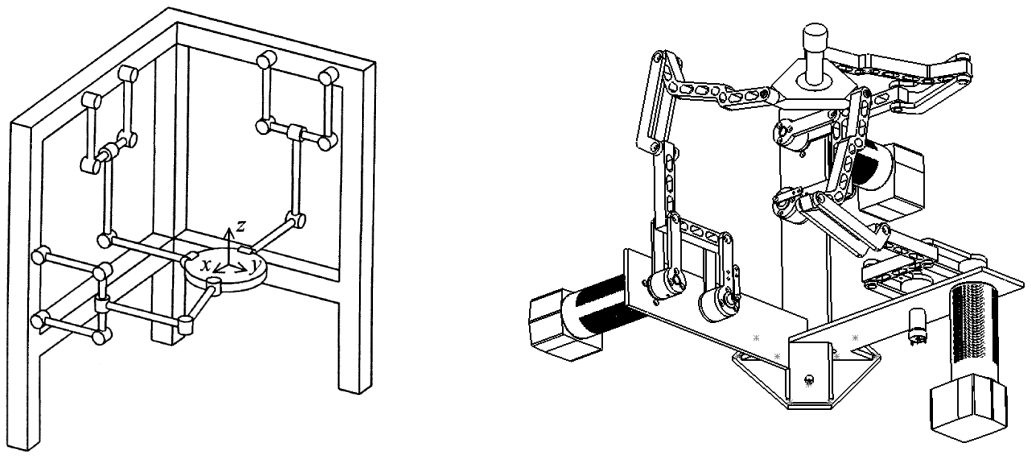

(a) (b)

Figure 4.9. R-CUBE designs: (a) Original design (Source: Li, et al. 2005), (b) Rotated design

In haptics, due to the random motion of the operator, motion through singular positions must be restricted. During the design procedure two singularity conditions are encountered which are important to avoid mechanically. One of them is already discussed in the work by Weimin Li, et al. 2009 and presented as avoidable with a proper design. The reported singularity is at at $\theta_i = \pm 90$ of the first link of the mechanism which is shown in Figure 4.10(a). Although the four-bar mechanisms are reported as possible engineering trouble by Weimin Li, et al, the problem is resolved by precise manufacturing technologies and the redundant constraint structure are used in order to avoid the singularity position mechanically (Figure 4.10(b)).

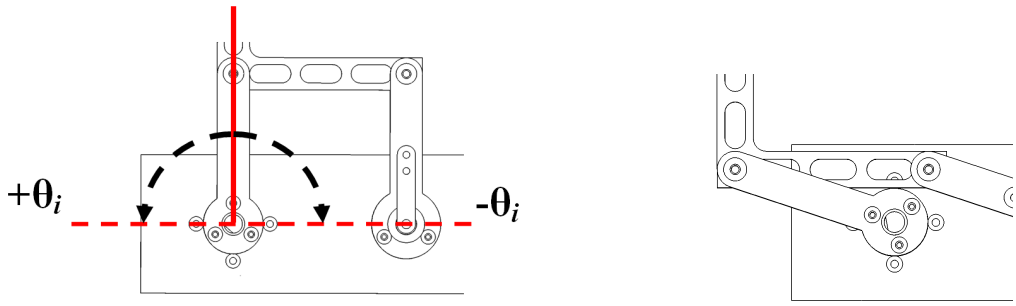

(a) (b)

Figure 4.10. Singularity in the first link: (a) Singularity if $\theta_i=\pm 90$, (b) Singularity avoidance

In Figure 4.11, the link lengths of the j^{th} link is denoted by l_{ij} for j=1, 2, 3, 4. The singularity at $\theta_4=0$ may cause trouble at the boundaries of the workspace. Hence the link lengths of the link, l_{ij} for j=2, 3, 4 are configured to avoid any link collisions and possible singularity positions. The link length determination process is based on the iterative simulations of the mechanism that were carried out in CosmosMotion©.

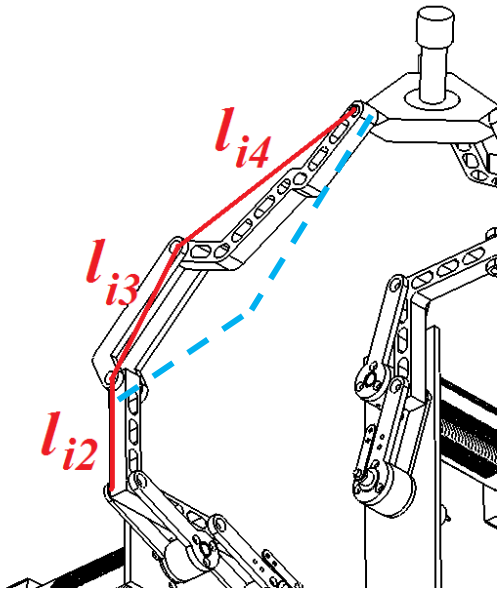

Figure 4.11. Length of the second, third and fourth links

The location of the workspace is important for the compactness of the design and it is limited with the footprint of the haptic device which is specified in the design criteria table (Table 4.1). The graphical representations of the workspace and S_i parameter which defines the distance of the actuation axis from the origin of the base

frame are shown in Figure 4.12. The location of the workspace is determined with S_i parameter by identification of the dimensional limitations of the mechanism.

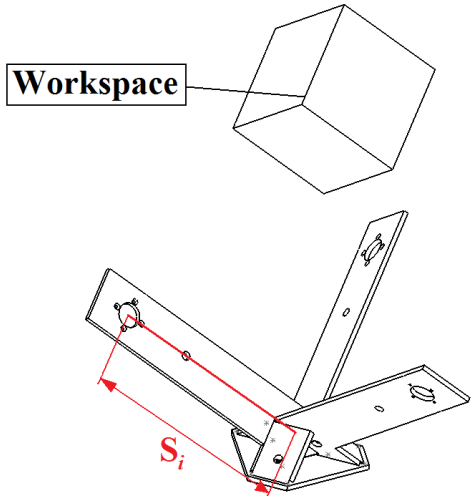

Figure 4.12. The workspace and the S_i parameter of the mechanism

Lengths of the first links (Figure 4.13) determine the volume of the workspace. According to the design criteria the first link length of the mechanism is calculated by direct kinematics analysis formula which is shown in detail, in Section 4.7, in order to meet the 120x120x120mm workspace specification.

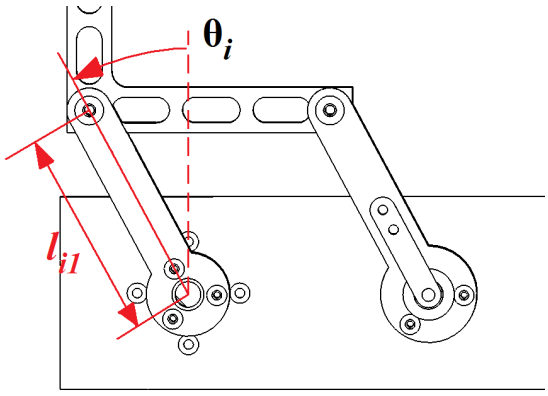

Figure 4.13. Joint variables and length of the first links

4.5.2. Component Design Criteria

The main criterion of the parallel mechanism is to develop a universal design that is appropriate for different types of orientation mechanisms, so the moving platform of the mechanism (Figure 4.14) is designed complying with this criterion. An example of this is presented in Figure 4.15 where instead of the orientation mechanism a simple handle mechanism is mounted on the platform thus the hybrid mechanism's total DOF is decreased to 3-DOF. Similarly, mounting a 4-DOF mechanism can result in a total 7-DOF hybrid structure.

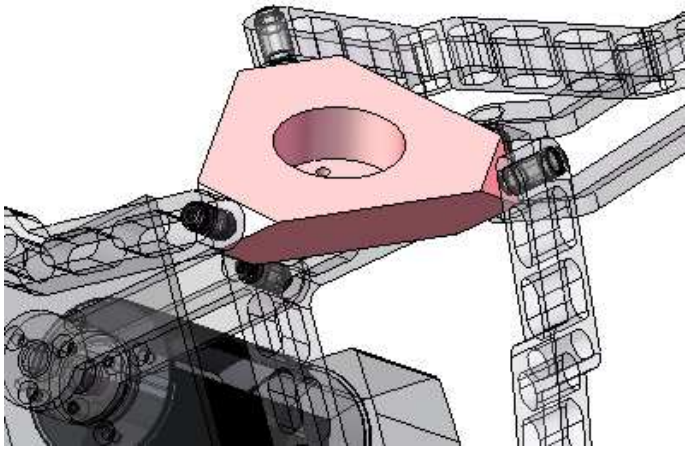

Figure 4.14. Platform of the mechanism

During the design of haptic desktop devices, one of the most important design specification is the handle space that is required for operator's hand to fit ergonomically, especially when converting a standard manipulator design into a haptic device. Therefore during the design of the final mechanism, the ergonomics of the handle space is also conceived in the design phase.

In the design, the locations of the sensors are selected for aesthetic considerations and to have a universal design for incorporating various sensor types. The three position sensors of the mechanism mounted at the base frame on the free rocker of the four-bar mechanisms as shown in Figure 4.15(a) denoted as 1, 2, 3. The position sensors of the mechanism can be replaced with various types of sensors only by remanufacturing the sensor housings. In Figure 4.15(b), the sensor mechanism is

shown with the sensor housing denoted as 1, the sensor as 2, the bearings as 3, and the shaft of the sensor as 4

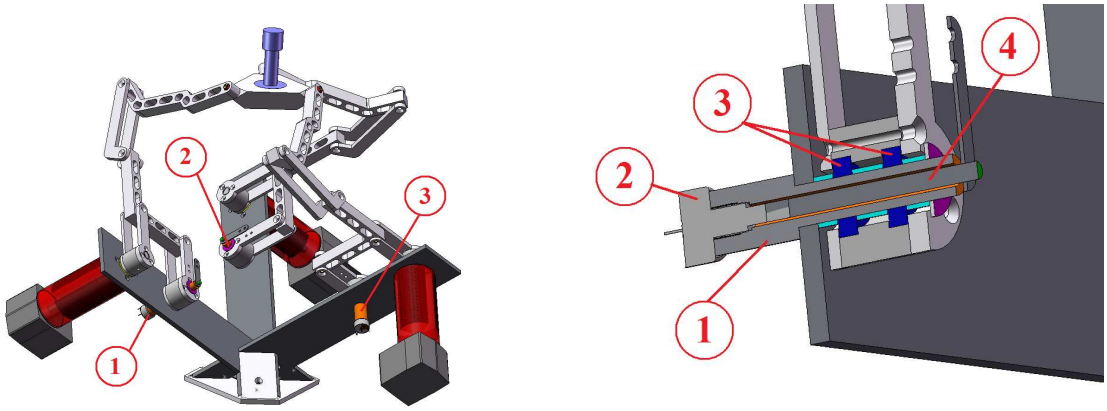

(a) (b)

Figure 4.15. Sensor locations and sensor housing designs: (a) Location of the sensors, (b) The design of the sensor housings

The CAD representation of the joint structure is shown in Figure 4.16. The structure has a shaft (4), bearings (3), screws (1) and the bearing plates (2). The outer bearing plates at the left and right hand side of the image are shown in the Figure 4.16. They provides leaning surface for the screws while fastening the joints. The inner bearing plate shown in the middle of the image prevents the outer races of bearings against getting stuck. The main objective in this design is to improve the mechanical precision of the joints. Besides it is also aimed to design a compact structure which has easy disassembling procedure.

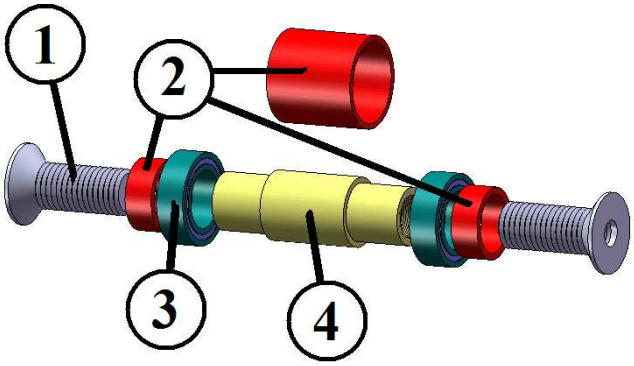

Figure 4.16. CAD representation of joint components M4 screw, bearings and bearing plates

4.5.3 Link Dimensioning and Shape Identification

Link dimensioning and shape identification of the translation mechanism are results of the structural and mechanical criteria outlined previously. The determination criteria can be listed as;

i) Dimensions of the workspace
ii) Location of the workspace
iii) Universal design
iv) Structure of the joints
v) User's handle space requirements
vi) Singularity avoidance

The lengths of the first links are determined to meet the workspace dimension specification. Previously defined 100x100x100mm workspace criterion is extended to 120x120x120mm, in order to avoid the motions in the close-range of the singular positions. The location of the workspace, which is important for the general dimensions of the mechanism, is identified with the max footprint criterion (Table 4.1). The universal design criterion sets the dimensions of the moving platform (Figure 4.14); therefore the dimensions are determined by the size of the possible upper mechanisms. Volumes of the links are minimized to decrease the weight of mechanism. The cross-sectional area of the links is determined through the dimensions of the joint structure (Figure 4.16). The second, third and the fourth link length and shape determination process is based on the iterative simulations carried out in SolidWorks© CosmosMotion© utilizing the singularity positions, link collisions and handle space ergonomics.

4.6. Design of the Final Orientation Mechanism

The serial structure proposed for the final design does not have any structural criteria. Therefore, link dimensioning and shape identification of the orientation mechanism's links is the result of criteria;

i) Sensation levels

ii) Ergonomic design

iii) Available sensors

Due to the manufacturing limitations and precision requirements, previously employed orientation mechanism of the prototype system is replaced with the serial-spherical manipulator in the final design. The orientation mechanism, serial-spherical manipulator is a 3-DOF-RRR spatial serial mechanism shown in Figure 4.17.

The mechanism is designed for monitoring the rotational motions of the user's hand, so it is designed in consideration with handle ergonomics. The design is manufactured in rapid prototyping machine in our laboratories and the ergonomics are tested (Figure 4.17).

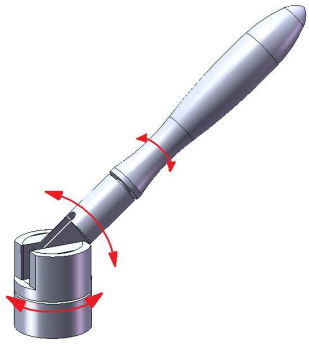

Figure 4.17. Orientation mechanism

The primary challenge in the design of this mechanism is adjusting the size of the mechanism with huge amount of components, such as position sensors, bearings, cables and A/D converters. 3-DOF rotational motions of the end-effector are monitored through three miniature sensors as shown in Figure 4.18 (b). The A/D converters are mounted inside the mechanism (Figure 4.18 (a)) in order to reduce the noise level by converting the analog outputs of the position sensors to digital signals.

(a) (b)

Figure 4.18. Position sensors: (a) Location of the sensors, (b) Dimensions

The design procedure of the mechanism is finished with necessary modifications to facilitate the manufacturing process. Finally, the model is designed in CAD environment and blue-prints are prepared for the test of the ergonomics of the mechanism. The CAD design of the new configuration of the hybrid mechanism with motors, sensors, bearings is shown in Figure 4.19. The manufacturing process is discussed in the following chapter.

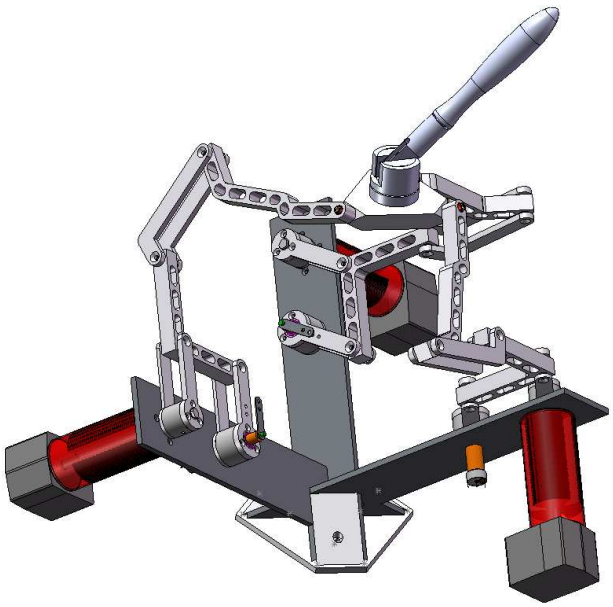

Figure 4.19. The CAD representation of the final design

4.7. Kinematics and Static Force Analysis

Haptic devices are the systems that are used to manipulate virtual or real systems that may be a virtual or a robotic arm. In order to control a virtual or real system by a haptic interface, the position of the handle point has to be measured then measured or calculated forces from the VR system or the slave side of the teleoperation must be reflected back to the operator. The position of the tip point, Wr, (Figure 4.20) must be calculated with direct kinematic analysis of the parallel mechanism (R-CUBE) making use of the joint sensor readings. Forces on the VR system or teleoperation slave system must be calculated or measured to restrain the operator's motion with calculated forces. In this section the position and torque calculation formulas of the developed haptic device are presented and discussed.

In Figure 4.20, position of the tip point, Wr, is defined as the intersection point of the last link connection surfaces on the moving platform. The origin of the base coordinate frame, O, is located at the intersection point of the unit vectors of the coordinate frame that is originated from the respective actuator axes. The mechanism parameters, variables and the rotated coordinate axes as shown in Figure 4.20 that are used in the direct and inverse kinematics analysis, and in the static torque calculations.

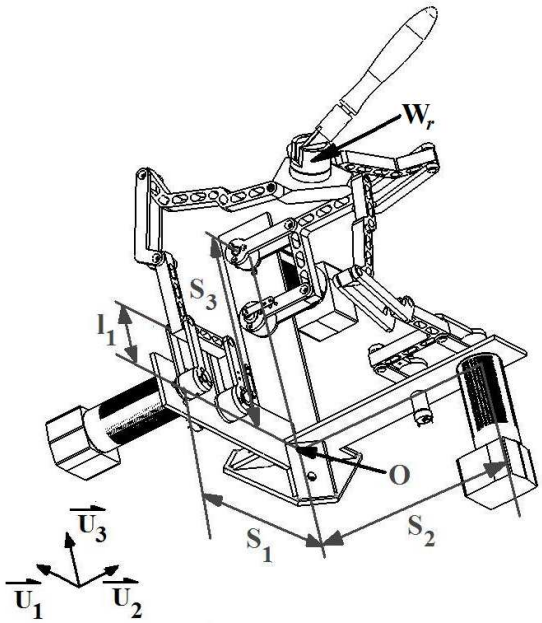

Figure 4.20 Mechanism parameters

In the parallel mechanism, the translational motion of the platform is regulated by the orientation of the actuators. Due to the decoupled motion of the mechanism, the motion along $\vec{u}_1$, $\vec{u}_2$ and $\vec{u}_3$ axes is only dependent on the motors placed on the same axes which have rotations about $\vec{u}_2$, $\vec{u}_3$ and $\vec{u}_1$ axes, respectively. Therefore, the mechanism's direct and inverse kinematics analysis is relatively trivial. Nevertheless, the mechanism is only decoupled in rotated coordinate frame as shown in Figure 4.20, hence the torque and position analysis of the system is carried out in rotated coordinate frame. For VR or teleoperation applications coordinate frame is reoriented with rotation sequence presented in Equations 4.1, 4.2 and 4.3. The reorientation angles, α and β, are calculated by using the isometric projection representation (Figure 4.21) (Carlbom and Paciorek 1978).

$$\hat{C}^{(R,W)} = e^{\tilde{u}_1 \alpha} e^{\tilde{u}_2 \beta} \tag{4.1}$$

$$\alpha = \arcsin(\tan 30°) \cong 35.26° \tag{4.2}$$

$$\beta = -45° \tag{4.3}$$

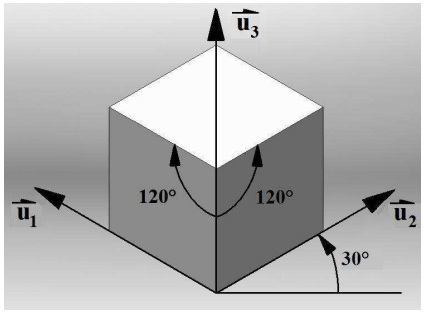

Figure 4.21 Isometric projection

The control scheme of the slave system is based on the calculation of the Wr point by utilizing the measurements from the positions sensors. This procedure is generally called direct kinematics. In the Equation 4.4, the calculation of the position vector of the tip point, Wr, with respect to the origin point, O, in the ground reference frame which is resented in Figure 4.20, is described.

$$\overrightarrow{Wr} = Wr_1\vec{u}_1 + Wr_2\vec{u}_2 + Wr_3\vec{u}_3 \tag{4.4}$$

Components of the Wr vector are a function of the rotation amounts of the actuators, θ, as shown in Equation 4.5. The zero position of the angle, θ_i, is represented with dotted line in Figure 4.22., In Equation 4.5; S_i is the distance between motor axes and origin point presented in Figure 4.20. l_i is the link length of the first link which is previously presented in Figure 4.20.

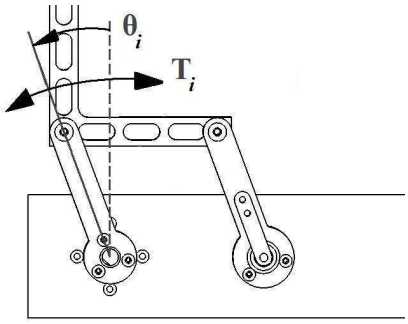

Figure 4.22. Joint variable (θ_i) and torque (T_i) directions

$$Wr_i = S_i + l_i \sin(\theta_i); \quad i = 1,2,3 \tag{4.5}$$

The inverse kinematics solution is given in Equations 4.7 and 4.8. In inverse kinematic solution, the mechanical structure of the four-bar mechanism limits the motion of the first link to about ±65°. Therefore, it is not possible to pass to the region where the cosines of the joint variables become negative. As a result of this, the sign ambiguity denoted with σ in Equation 4.7 can be neglected and σ can be taken as +1 without the loss of generality.

$$\sin(\theta_i) = \frac{Wr_i - S_i}{l_i} \quad i = 1,2,3 \tag{4.6}$$

$$\cos(\theta_i) = \sigma\sqrt{1-\sin^2(\theta_i)}; \quad \sigma = \pm 1 \tag{4.7}$$

$$\theta_i = \arctan_2(\sin(\theta_i), \cos(\theta_i)) \tag{4.8}$$

The components of the applied force, F, are calculated in the ground reference frame in Equation. 4.9.

$$\vec{F} = F_1\vec{u}_1 + F_2\vec{u}_2 + F_3\vec{u}_3 \tag{4.9}$$

Torque demands for a specified force that has to be applied to the operator's hand can be formulated by Equation 4.10. In Equation 4.10, T is the torque required to be applied by the actuators about their respective axis of rotation as shown in Figure 4.22, and F is the desired force to be applied to the operator's hand. Torque values for each actuator are calculated by taking cross product of the moment arm vector, Wr, and the force vector, F, and then taking the dot product with the respective actuator's rotation axis. The torque element in all axes that has the moment arm along its respective axis is neglected because the forces will not be transferred as a consequence of the rotation axis arrangement of links 2, 3, and 4. T is the torque applied by the actuator about each axis as shown in Figure 4.20, and F is desired force to be applied to the operator's hand.

$$\begin{aligned} T_1 &= F_1(Wr_3) \\ T_2 &= F_2(Wr_1) \\ T_3 &= F_3(Wr_2) \end{aligned} \tag{4.10}$$

In Figure 4.23, the tip point of the parallel mechanism is denoted with Wr. The orientation mechanism is in the form of a spherical wrist configuration. Thus, its forward kinematic analysis is provided as a series of pure rotations as in Equation 4.11. The orientation mechanism is a passive mechanism. The inverse kinematics solution is not required since the motion of the mechanism is not controlled by any actuation system. The measured angles from this mechanism are used only for the control of the rotation motion in VR or teleoperation applications.

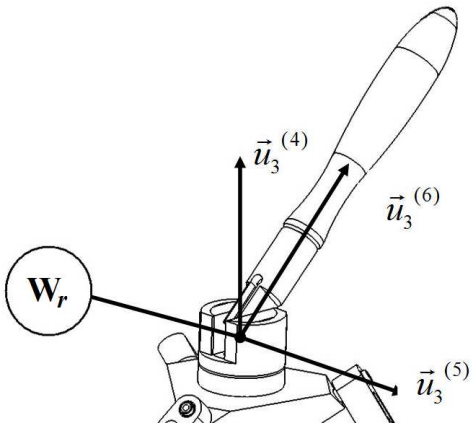

Figure 4.23. Wr point of the mechanism

$$\hat{C}^{(3,6)} = e^{\tilde{u}_3\theta_4} e^{\tilde{u}_2\theta_5} e^{\tilde{u}_3\theta_6} \tag{4.11}$$

CHAPTER 5

MANUFACTURING PROCESS

5.1. Introduction

The designed device is manufactured by utilizing various types of manufacturing processes, such as wire erosion, laser cutting, milling and turning for both translation and orientation mechanism. In general the manufacturing process of the entire mechanism is challenging due to;

i) Small scale parts
ii) High precision parts
iii) Parallel structure
iv) Irregular part shapes
v) Non-magnetic materials
vi) Average machinability materials

The design of the mechanism includes small bearings, bearing housings, bearing shafts, wiring and electronic component houses which are difficult to manufacture with conventional manufacturing processes. All moving parts of the mechanism are manufactured with high precision in order to detain possible backlashes and develop high precision mechanism. Nonidentical and less precise parts in a parallel mechanism can also block the motion of the mechanism. As a result of the link length and shape determination process outlined in section 4.5, the manufacturing of the irregular shaped parts result in a difficult and long manufacturing process. Especially, the platform of the mechanism is manufactured in several manufacturing phases. The presented materials which are discussed in the next section have average machinability and non-magnetic atomic configuration. In general magnetic materials can be clutched with magnetic clutches to the milling and turning machines, however non-magnetic materials require custom manufactured fixture in order to fix the

workpiece to the machines. Manufacturing the parts of the mechanism with custom gages and fixtures increases the cost and time of the manufacturing process.

In this chapter the steps of the manufacturing process are presented and explained with figures.

5.2. Material Selection

In material selection for translational mechanism, the primary objectives are to manufacture the mechanism with a material that is light, non-corrosive, and rigid. Therefore, non-ferrous metal alloys based on aluminium, zinc, nickel, copper, titanium, tungsten and cobalt are investigated and among the other non-ferrous alloys aluminium alloy 7075 is used to manufacture of the parallel mechanism. 7075 aluminium alloy includes 5.1-6.1% zinc, 2.1-2.9% magnesium, 1.2-2.0% copper, maximum 0.4% iron, less than 0.4% silicon and other metals. Its density is about 0.0028 g/mm³ and it has wide application in highly stressed structural parts that range from various commercial aircraft components, aerospace to defence equipments. The material combines high strength with moderate toughness and corrosion resistance. Alloy 7075 offers reasonable price and good machinability when machined with carbide machining tools.

The primary objective during the material selection of the orientation mechanism is to use ultra light materials, in order to reduce the payload amount of the platform of the mechanism. An engineering plastic, cast polyamide commonly known as Kestamid© can provide low densities with reasonable rigidity and price. Delrin material has density about 0.0014 g/mm³ and it has wide application for general purposes especially in chemical and food industries. It is resistant to corrosion and it has average machinability.

5.3. Manufacturing Process of Translation Mechanism

The manufacturing process of the translation mechanism initialized with the manufacturing of the base frame is shown in Figure 5.1. Different from the other components of the translational mechanism, the base frame is manufactured with sheet stainless steel because of the high strength requirements. The base frame is the chassis

of the mechanism; it carries the actuators, sensors and the mechanism. Therefore its dimensions have to be accurate. Among the other sheet metal cutting technologies more precise laser cutting technology is used for the manufacturing of the parts. The parts of the base frame and the assembled frame can be seen in Figure 5.1(a) and Figure 5.1(b), relatively.

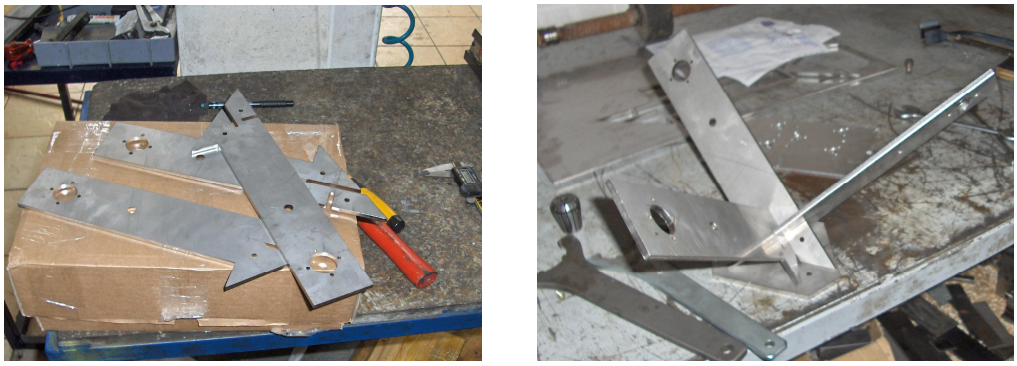

(a) (b)

Figure 5.1. Base frame of the mechanism: (a) Parts, (b) Assembled structure

The sliding joints of the prototype mechanism are replaced with roller-bearing joints in the recent mechanism to be able to prevent possible backlashes. In the joints, bearings that have 8mm outer and 5mm inner diameter with 3 mm width are used. For such a small scale roller-bearings, small scale shafts (Figure 5.2(a)) and bearing houses are manufactured. The shafts are manufactured by CNC turning machines from brass for its good strength and corrosion resistance properties (Figure 5.2(b)). M4 screw thread is cut inside of the shaft for fastening the joints.

(a) (b)

Figure 5.2. Shafts of the mechanism: (a) CAD representation of shafts with M4 screw thread, (b) View of the bearings on shaft

During the manufacturing process of the translation mechanism the principal technique is the wire-erosion machining. Wire-erosion machining is a modern machining process, based on material removal technology with rapid electrical discharges. It has the capability to manufacture the complex shapes from very hard material with smaller tolerances. It also allows manufacturing of very small workpieces which is not possible with conventional tools. Therefore, most of the precise parts are fabricated with this process. Wire-erosion machine can be seen in Figure 5.3 during the manufacturing process of the links.

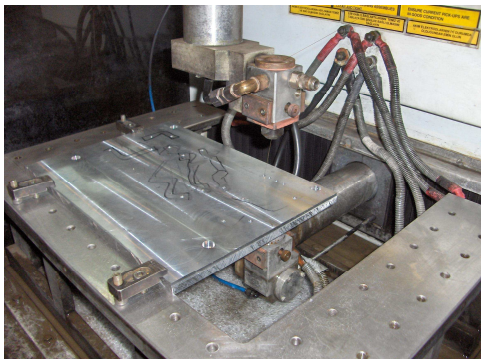

Figure 5.3. Wire-erosion machine

The bearing plates are small parts that have 6.2mm outer and 5mm inner diameter. In order to manufacture such precise parts, 7075 aluminium plate, with wire-erosion. The manufactured parts and assembled compact design of the joint can be seen in Figures 5.4(a) and 5.4(b), respectively.

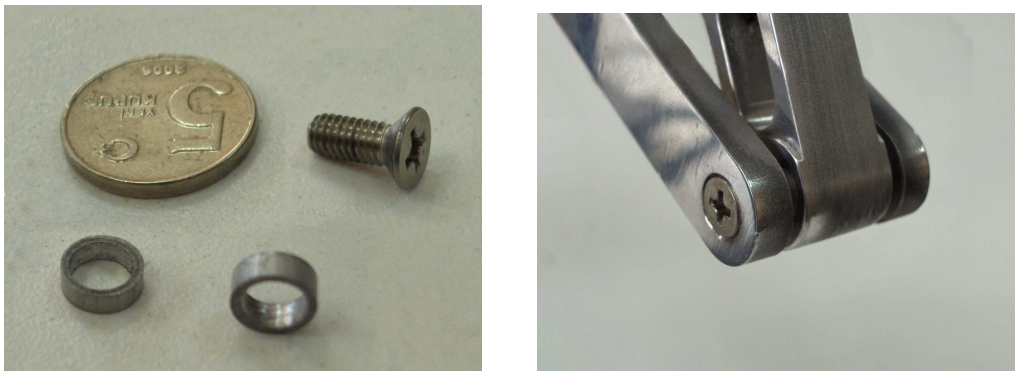

(a) (b)

Figure 5.4. Links of the mechanism: (a) Bearing plates, (b) View of the joint

The manufacturing of the bearing houses are one of the most demanding process in the mechanism. The axes of the joints must be parallel and identical to result in smooth joint motions. The bearing houses are cut during the manufacturing of the links then the holes are widened with drilling followed reaming process to meet the bearing tolerance specifications. The entire process is accomplished with custom designed and fabricated gage shown in Figure 5.5.

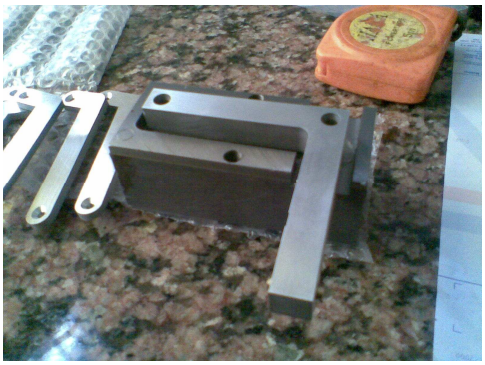

Figure 5.5. Custom gage for bearing houses

The links 1 and 2 are manufactured with wire-erosion from, 5mm, 7075 aluminium sheet metal and then the process is finished with counter-sinking. The manufactured link 1 and 3 can be seen in Figures 5.6(a) and 5.6(b), respectively

(a)

(b)

Figure 5.6. Links of the mechanism: (a) Link 1, (b) Link 3

Other links, 2 and 4 is also manufactured with wire-erosion from, 14mm, 7075 aluminium plate. In the second step, the bearing houses are completed and finally, all links are perforated in order to decrease the weight of the links. The perforated view of

the fourth link and an assembled leg of the mechanism can be seen in Figure 5.7(a) and Figure 5.7(b).

(a) (b)

Figure 5.7. Links of the mechanism: (a) Link 4, (b) Assembled links

The moving platform of the mechanism is manufactured by CNC milling from 7075 aluminium billet. Among the other parts of the mechanism, this part has the most challenging manufacturing process due to its irregular shape and accuracy requirements. The geometry of the part is based on the modification of a cube; partiality shown in Figure 5.8(a) and 5.10(a). The surfaces of the cube have to be parallel and the cube must provide high fidelity geometry. Therefore the manufacturing process is started with fabrication of a uniform cube that has approximately ±0.001 tolerance range (Figure 5.8(b)).

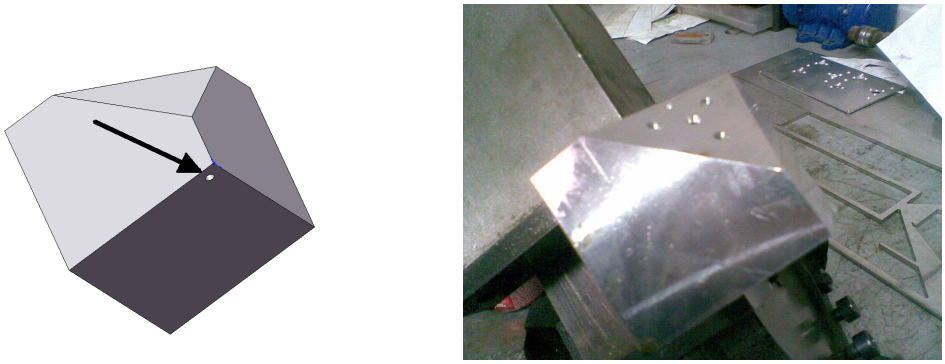

(a) (b)

Figure 5.8. Manufacturing process of Link5: (a) CAD representation of first edge removing, (b) Manufacturing process of first edge removing

The three screw holes for the joints are perforated as shown in Figure 5.8(a). Afterwards the workpiece is rotated about α, and β (Equation 4.2, 4.3) by bevel protractor and the one edge of the cube is removed as shown in Figure 5.8(b).

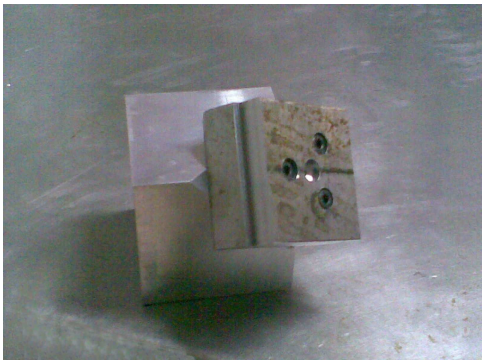

Figure 5.9. Custom fixture for link 5

The other edge of the link is removed with custom fixture shown in Figure 5.9 and the manufacturing process can be seen in Figure 4.10(b) by milling machine. Created surfaces are not the working face. Therefore the precision of the edge removing process is not important.

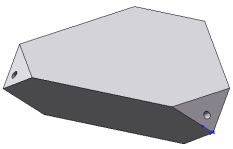

(a) (b)

Figure 5.10. Manufacturing process of Link5: (a) CAD representation of second edge removing, (b) Manufacturing process of second edge removing

Finished moving platform of the mechanism from aluminium alloy 7075 can be seen in Figure 5.11. The part is also manufactured from polyoxymethylene plastic (delrin) material by the same manufacturing processes in order to reduce the total payload.

The manufacturing process of all links and the base of the mechanism are finished with polishing process to acquire clear surface. Then, inserts (Helicoil©) are threaded into the pre-taped holes to provide a more enduring threaded screw holes.

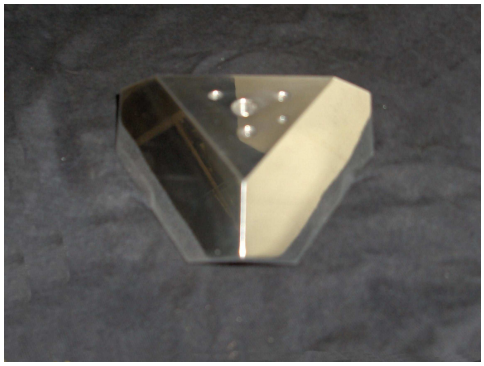

Figure 5.11. Finished platform of the mechanism

5.4. Manufacturing Processes of Orientation Mechanism

The orientation mechanism is manufactured utilizing turning process and hand workmanship process with Dremel©. The precision of the mechanism and the strength of the structure are relatively less significant than the lower mechanism because the structure has no active joints. It is a composed of four main parts as shown in Figure 5.12. In Figure 5.12 base link denoted as “1”, the first link as “2”, the second link as “3”, and the third link as “4”

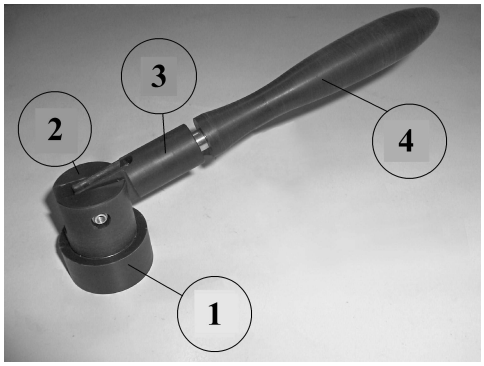

Figure 5.12. Orientation Mechanism

The base of the mechanism is used to fix the orientation mechanism to translation mechanism. It is manufactured from kestamid© by turning. The

manufacturing process is simple since it contains only a sensor house and bearing house. The manufactured base link can be seen in Figure 5.13.

Figure 5.13. Base of the orientation mechanism

The first link of the mechanism is shown in right hand side of the Figure 5.14(b), it is manufactured from kestamid© by turning and hand workmanship process. It includes bearing surfaces for the first and the second axes and sensor housing. It has also simple manufacturing process except for the wire ways that can be seen in Figure 5.14(a).

(a) (b)

Figure 5.14. Link 1: CAD representation of link 1, (b) Link 1 and link 2

The second link can be seen in the left hand side of the Figure 5.14(b). The components (Figure 5.16(a)) of the third axis are squeezed in a small volume which is partially shown in Figure 5.15. The link is the most complicated part in the orientation mechanism. Therefore the manufacturing process is long and difficult. Especially,

manufacturing the miniaturize potentiometer house is a result of multiple trials. It is manufactured from Kestamid© by turning, milling and hand workmanship process.

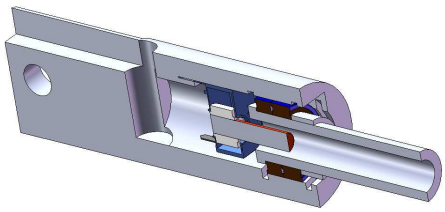

Figure 5.15. CAD representation of link 2

The last link of the mechanism is shown in Figure 5.16(b). It does not include any mechanics or electronics. It is the handle part of the joystick so it is designed considering the ergonomics. The manufacturing of this link is also difficult due to the dimensions and the plastic material. It has about 130mm length and 15mm pitch diameter which causes workpiece vibrations during the milling process. Hence the milling process is accomplished in multiple trials.

(a) (b)

Figure 5.16. Link 3: (a) Shaft and bearings, (b) Link 3

5.5. Conclusion

The manufacturing processes of the mechanisms are presented in this chapter. Even though the manufacturing process is challenging due to the, non-magnetic materials, irregular part shapes and small scale high precision parts, precise manufacturing processes, such as wire erosion, laser cutting, CNC milling and turning made the manufacturing of the parts possible. The tests of the assembled translation mechanism (Figure 5.17) show that the mechanism does not have any structural problems. Links and the joints of the system have low frictional loss and provide smooth joint motions which are important to provide higher level of sensations.

Figure 5.17. Assembled translation mechanism

The orientation mechanism (Figure 5.17) also has smooth joint motions and low frictional loss. It does not have any structural problems, but it has some bearing problems which is discussed in the following chapters.

Figure 5.17. Assembled orientation mechanism

In the next chapter, integration of the mechanism with electronic and electro-mechanic components of the system is explained and the properties of them are presented.

CHAPTER 6

INTEGRATION OF THE SYSTEM

6.1. Introduction

Haptic systems are composed of mechanical, electro-mechanical and electronic components. The mechanical component of the system is presented and manufacturing processes are explained in the previous chapters. The electronics and electro-mechanical components such as actuators, sensors, data acquisition cards and motor amplifiers of the system are required to be selected and integrated to the system. In this chapter, the selection of the outlined components of the system is discussed and selected components are presented. The integrated system is tested and according to initial tests result, necessary design changes is identified and applied.

6.2. Data Flow Through the System

The basic components and the data flow among these components are shown in Figure 6.1. This flow chart facilitates the identification of the correlation and data transfer between the system and the components. The control scheme of impedance type haptic system starts with the measurement of the positions of the mechanism's degrees of freedom from potentiometers via data acquisition card. The analog signals from the potentiometer are converted to digital signals by ADCs in the DAQ card. Through the reserved communication port of the PC, digital signals are transferred to the computer control software and the forces are calculated as a result of the interaction between the object and the environment in VR or teleoperation application. Afterwards, the resultant forces are transmitted back though the same way, back to the actuators of the mechanism. In a VR application, acquired signals from the motion sensors through the DAQ card are used to move a virtual object in VR screen.

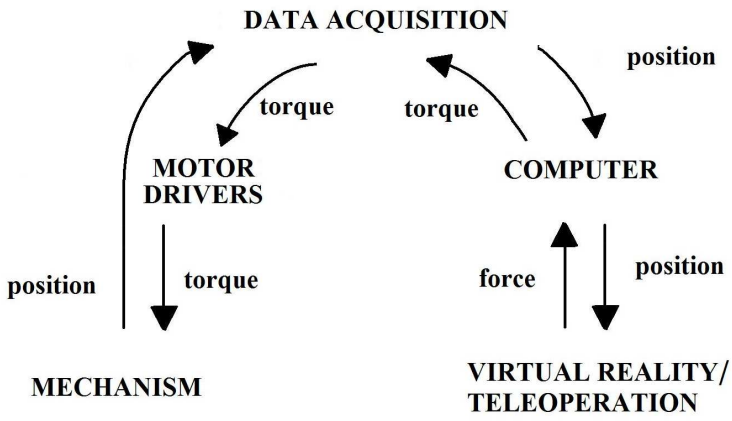

Figure 6.1. Data flow

The only difference in teleoperation integration of this haptic device would be that actual forces has to be measured on the slave side of teleoperation instead of calculating virtual forces in the VR environment. The slave system is usually at a distant site. Therefore, the signals between the master and the slave robot must have a communication system such as the Internet, cables or wireless technology in teleoperation systems.

6.3. Motor, Drive System and Motor Amplifier Selection

Among the other actuation methods presented in the Chapter 2, DC motors are the most frequently used actuator types in the design of the robotic applications owing to their simple structure, low cost, high reliability and wide availability for various applications. DC motors are also used in the design of the haptic devices. In this thesis due to their advantages outlined above, Brushless DC motors are employed in the system. Basically DC motors can be grouped in two categories as brushed and brushless DC motors. Brushed DC motors are composed of brushes, commutator, stator and rotor. Because of the switching mechanism, motor and the maintenance cost of the actuator is high and the structure of the motor is sensitive to dust and abrasion. In contrast brushless DC (BLDC) motors include only a permanent magnet rotor and a stator. In BLDCs, the switching is generated with electronic switching circuits, instead of any mechanical switching. The advantages of the brushless DC motors can be listed as

i) Includes fewer components that result in simple structure and low inertia.

ii) Low maintenance requirements and long life.

iii) High efficiency.

iv) Reduced motor length and compact design.

v) Low switching noise.

The disadvantages of the brushless dc motor configuration relative to the brushed DC motors are;

i) Relatively high cost due to the cost of the permanent magnet.

ii) Do not include any shaft for position sensing.

iii) Complexity in the electronic controller.

The actuators are selected as a result of the force analysis performed in the CAD simulations. The applied force specification is to apply at least 0.8 N of force in all directions. This specification is consistent with the similar haptic devices in the market (www.sensable.com). The initial selection of the actuator is a Maxon brushless DC motor that provides 310 mNm of continuous torque according to its datasheet (Figure 6.2).

Figure 6.2. Selected maxon motor

In haptic devices, usually DC motors with capstan drives are used. However, it is foreseen that in time, the cables of the capstan drives loosen and results in loss of

precision since the mechanism is driven without any transmission mechanism. Brushless dc motors are used in direct drive formation.

The system requires motor amplifiers that drive the three BLDC motors through current mode requiring +/- 10 V analogue signals as inputs. Maxon brushless dc motor amplifiers (drivers) are selected to be compatible with the current requirements of the motors. These amplifiers are used to drive the actuators in current mode can be seen in Figure 6.3, which enables to drive the actuators by torque inputs that originated from the haptic controller system. The amplifiers are selected to have a response rate of at least 1 kHz.

Figure 6.3. Selected maxon motor amplifier

6.4. Sensor Selection and Integration

The design of the mechanism allows using separate sensors to measure the rotation amount of each actuator. Thus, it is not required to have an encoder system at the rear end of the actuator which usually has 9-bit of resolution. The four-bar structure placed as the fist link has identical nominal lengths, which permits the same motion on each link.

Figure 6.4. Selected position sensors

A potentiometer or a higher bit resolution encoder (12-bit) can be aligned with the free link of the four-bar system and measure the same motion with more precision. In the initial system, six potentiometers that provide analogue signals, three on the parallel mechanism and three on the orientation mechanism, are used due to their low cost and simplicity. The selected potentiometer (Figure 6.4) for the links of translation mechanism has linear track tapper, approximately 270^{o} mechanical angle, ±5 resistance tolerance and 1% linearity error. In order to design a compact handle mechanism, it is required to use miniaturize potentiometers.

The potentiometers of the rotational mechanism (Figure 6.5(a)) have small dimensions about 10x11x4 mm. Although the presented components, called trimpot, are not designed for position sensing, due to the availability limitations of miniaturize size position sensors, these trimpots are used as sensors.

(a) (b)

Figure 6.5. Sensing the position of the orientation mechanism: (a) Miniaturize sensors, (b) ADC and passive components

In order to minimize noise in the analog signal it is required to convert to digital signals directly. Therefore 16-Bit, High-Speed, ADC ADS8331 (Figure 6.5(b)) and the passive filtering components are mounted on the back of the trimpots as shown in Figure 6.6(a). Finally the integrated sensor modules are placed into the links of the mechanism. Located sensor of the second link can be seen in Figure 6.6.

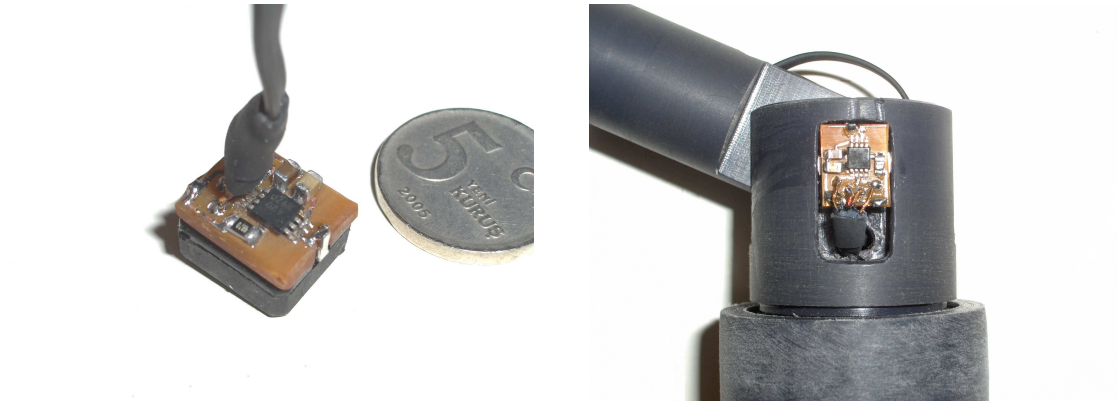

(a) (b)

Figure 6.6. Integration of the miniaturize position sensors: (a) Integrated sensors, (b) Sensors on the second joint of the mechanism

Due to the noise effects in high speed digital signals, cased ribbon cable is used for the power and data transmission between the integrated sensors and DAQ card (Figure 6.9). Other types of digital signal cables are also tried such as standard ribbon cables but positive results can be taken. Moreover the array of the signal cables are also important, the data, clock, positive supply, ground and enable signal cables are denotes as 1, 2, 3, 4, and 5 respectively in Figure 6.7.

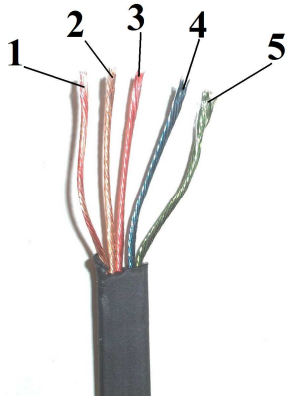

Figure 6.7. Cased ribbon cable DAC data converter

6.5. Custom Data Acquisition System Design

A data acquisition (DAQ) card is used to convert analogue inputs from the potentiometers to digital signals to be fed into the computer and digital outputs from the computer to analogue signals to be fed into the motor amplifiers.

This thesis also comprises an experimental study about design and development of a custom data acquisition system. The developed data acquisition card is Microchip© PIC based system that has six 16-bit A/D converters and three 16-bit D/A converters. The developed data acquisition system includes three analog to digital converter, micro processor, three digital to analog converters and RS-232 communication ports denoted with 1, 2, 3, and 4, which can be seen, respectively in Figure 6.8.

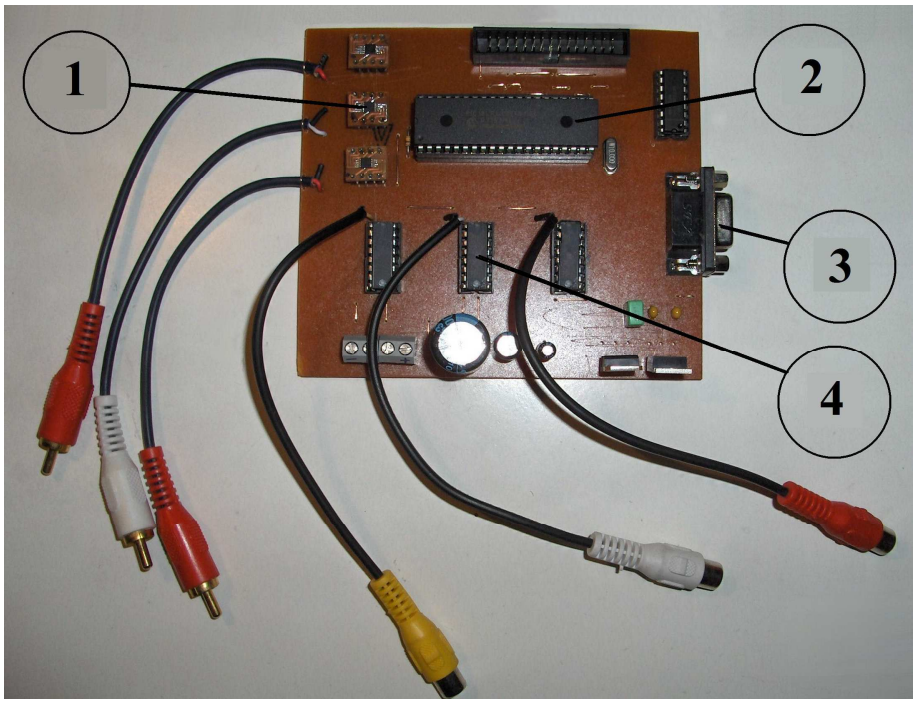

Figure 6.8. Custom data acquisition system

6.5.1 The Components of the Custom Data Acquisition

The important components of the developed data acquisition system can be listed as microprocessor, analog to digital converter and digital to analog converter units. The selected microprocessor of the system is PIC18f4431; this midlevel

microchip provides good performance with reasonable prices. It support clock speeds up to 40MHz, it has 16384 bytes program memory, 768 bytes of data memory and high-speed 10-bit A/D converters. Moreover it also provides quadrature encoder interface which could be used for optical sensing operations in the later versions of the developed haptic device.

The ADCs of the system is a product of Burr-Brown which can be seen in Figure 6.9.The ADS8320 is a 16-bit ADC that provides 100 kHz sampling rates via synchronous serial communication protocol. It has very low power requirements and differential input. The ultra-small package size (MSOP-8) of the ADS8320 makes it ideal for compact data acquisition applications.

Figure 6.9. Selected analog to digital converter

The DAC714 is a low noise digital to analog converter that can provide ±10 volt voltage output without any additional opamps. It has high-speed synchronous serial communication interface which can operate in parallel bus connection, cascaded serial bus connection with asynchronous and synchronous update. The output pin is protected against possible short circuits to ground and the reference pins allow offset and gain adjustment. DAC714 is available in a plastic DIP16 package which can be seen Figure 6.10.

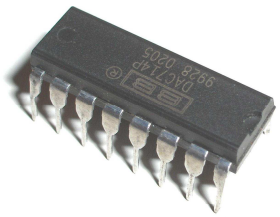

Figure 6.10. Selected digital to analog converter

The developed data acquisition card is employed and tested in Matlab© Simulink via serial port communication blocks in time and frequency domain applications. Nevertheless, the initial tests show that the developed data acquisition system can support up to 100 Hz of sampling rate which is not usually enough in haptic applications.

6.6. Commercial Data Acquisition System Selection and Integration

Although various types of commercial data acquisition systems are available, due to the performance ratings, Quanser Q8 Hardware in the Loop (HIL) Board from Quanser Consulting Inc. is selected. Q8 has eight 12-bit D/A converters, eight 14-bit A/D converters whivh is enough for 6-DOF mechanism. Furthermore, it also has eight quadrature encoder inputs is for future modifications on the system's sensors. The system currently occupies three D/A converters for motor amplifiers and six A/D converters for the potentiometers of the Q8. While human motion is limited to 10 Hz, forces that are up to 1 kHz is important for the perception of the outer media. Therefore, in general, haptic devices are required to have at least 1 kHz (Akahane et al. 2005) of sampling rate in order to accurately provide the sense of touch. Quanser Q8 can operate at 100 kHz sampling rates even in simultaneous acquisition.

Table 6.1. Specifications of Quanser Q8 DAQ Card

Analog Inputs	8x14-bit
Analog Outputs	8x12-bit
Quadrature Encoder Inputs	x8
I/O Channels	32xProgrammable
Dedicated Counter/Timers	2x 32-bit
Reconfigurable Encoder Counter/Timers	2x 24-bit
PWM outputs	x2
PCI bus interface	32-bit, 33 MHz

Due to the limitations of the developed custom data acquisition card (Figure 6.7), the initial tests of the mechanism are performed with the purchased commercial DAQ system. Nevertheless the small dimensions and wire houses (Figure 5.14(a)) transmitting the analog sensory outputs from the mechanism are impossible. Therefore the digital signals from the embedded DAQ components (Figure 6.6) are converted by the use of ADC to DAC converter circuit which can be seen in Figure 6.11.

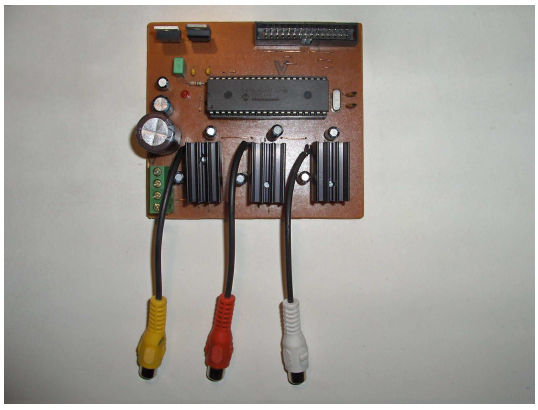

Figure 6.11. ADC to DAC data converter

In custom DAQ card the primary delays are the result of limited transfer rates of the serial port, so despite the designed circuit is also includes the same components with the presented custom DAQ system, it can operate within the desired frequencies.

6.7. Initial Tests and Modifications

The integrated system is tested and necessary design modifications are identified and some of them are applied system. According to the integrated system test results, necessary modifications are addressed in;

i) Rotation of the mechanism
ii) Motor selection
iii) Sensor selection
iv) Second link of the orientation mechanism

The initial test results revealed that the reoriented mechanism (Figure 4.9(b)) increased power consumption with respect to the original configuration (Figure 4.8) as shown in Table 6.2. Hence the orientation of the translation mechanism is changed back to the previous configuration (Figure 6.13).

Figure 6.12. Modified 6-DOF mechanism

Table 6.2. Max Power Consumptions for Gravitational Effects

	Motor No	Ampere
Reoriented Configuration	1	4.2
	2	4.21
	3	4.35
Original Configuration	1	0
	2	4.81
	3	0.8

Although the technical specification sheet of the selected rate presents the motor's stall torque at 310 mNm, it is measured that the actuator can apply one third of the rated stall torque. Furthermore, changing back the orientation of the mechanism decreased the force feedback capability. Nevertheless this configuration can still provides enough torque rates to the mechanism. In order to achieve the required the feedback capacity more powerful brushed dc motors are planned to be used.

Initially selected analog position sensors (potentiometers) provide noisy data which can results in precision loss. Therefore 12-bit three-channel incremental optical sensors (Figure 6.12) can be replaced far the potentiometers.

Figure 6.13. Selected optical encoder

The bearings and sensor installation track of the second link of the orientation mechanism is denoted respectively with 1 and 2 in Figure 6.14. The installation track is necessary for the installation of the DAQ module of the last link, however the deficiency in the sensor houses results in serious backlash on the handle mechanism. So the design of the link has to be modified.

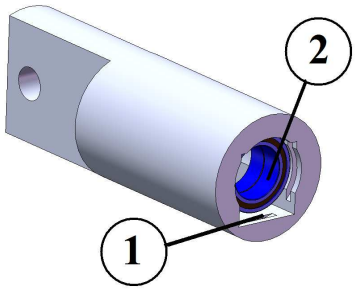

Figure 6.14. Second link of the orientation mechanism

6.8. Conclusion

In this chapter, the integration of the mechanism with the electro-mechanic and the electronic components are presented. Data flow among the system components is explained and the specifications of the system components are presented. Considering the initial test results, the necessary modifications are listed.

Integrated mechanism can be seen in Figure 6.14. The VR application, computer control scheme, DAQ components and the mechanism is denoted by 1, 2, 3, 4 in Figure 6.14, respectively

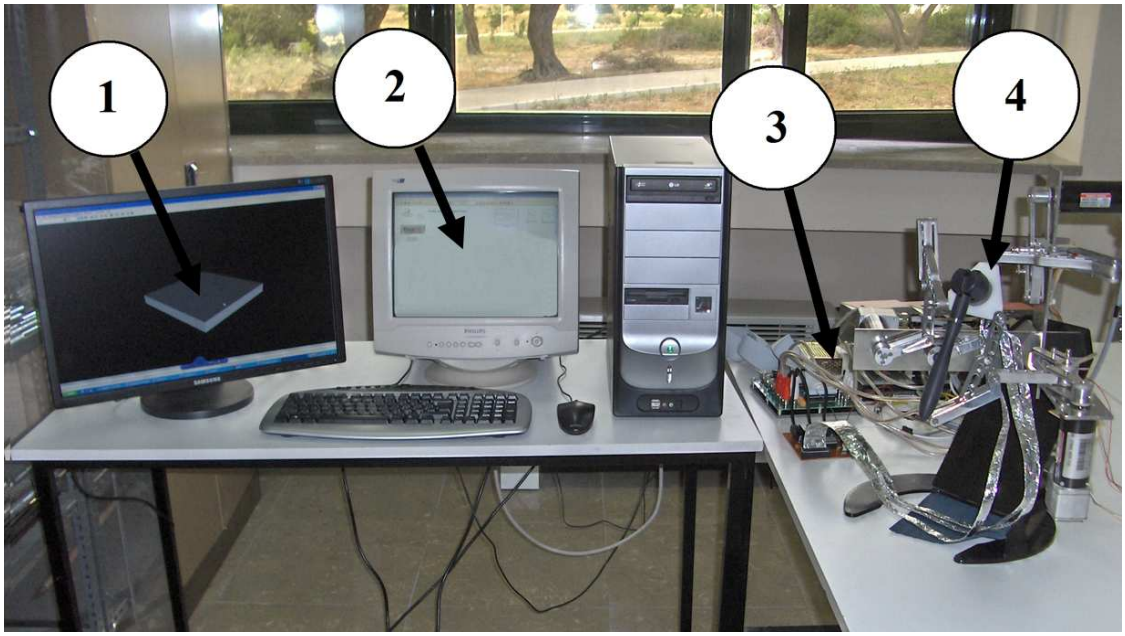

Figure 6.14. The 6-DOF haptic system

CHAPTER 7

CONCLUSIONS

7.1. Conclusions

The aim of this thesis is to develop a general purpose haptic device that provides higher precision ratings. Hence, previous haptic device designs are investigated, current haptic systems' sensation types are reviewed, mechanisms and their structural advantages are identified and haptic applications are grouped as teleoperation and VR haptics. Afterwards, the general haptic device components are listed and previously employed materials are reviewed. The difference of the admittance and impedance haptic devices is described, and drive systems are investigated according to the type of the haptic device. Some of the commercially available DAQ systems along with the custom DAQ systems are presented. Finally graphical DAQ software development languages are presented and compared to configure initial test environment making use of VR technology.

Towards developing a haptic device, the design phases of the mechanical part of the system are clarified. According to the defined design phases, the design criteria are identified and the conceptual designs are formed. Evaluating the literature survey results and the developed conceptual designs, R-CUBE mechanism is selected for reflecting three-dimensional forces and 3R serial spatial mechanism is selected for monitoring the orientation of the operator's hand. The selected mechanisms are configured as a haptic device and the dimensions and shapes of the links are determined to meet the specified design criteria. The designed mechanism is modified according to the manufacturing abilities, and then the mechanism is manufactured utilizing various manufacturing processes. The important points of the manufacturing process are presented and discussed.

The mechanical, electro-mechanical, electronics and software parts of the device are integrated. Considering the force feedback requirements, motors are selected along with the appropriate motor amplifiers. In order to improve the precision of the actuation system, the driving type is determined as direct drive. The sensors of

the system are identified and the orientation mechanism is integrated with its DAQ modules. Experimental studies on the custom DAQ card are performed and appropriate commercial DAQ system is selected and purchased. Then, the commercial DAQ system is integrated with the other components of the mechanism. Finally initial tests are performed, necessary design changes are offered and some of them are applied into the system.

7.2. Future Works

Haptic system development phases can be listed in three groups; the design and manufacturing the mechanical structure, development of data acquisition cards and the development of VR or teleoperation application. Until now, the structural development of the system is completed satisfying the precision requirements, experimental DAQ system is developed and tested and experimental VR is created in Matlab Simulink.

In the future the mechanism can be remanufactured with composite material in order to improve the weight/strength ratio. The electro-mechanical components such as sensors and actuators can be replaced for better accuracy and force ratings. . Hence, the potentiometers can be replaced with optical encoders and the motors of the system can be changed with other types of actuators such as coreless DC motors. Furthermore passive actuators can be integrated to the existing device; the four-bar mechanism provides unique advantage for such an implementation. The developed custom DAQ card's sampling rate can be improved with the use of more advanced technologies such as DSPs and FPGAs. VR application can be enhanced with better VR modules or custom programming. Moreover the system can be configured as the master system of a teleoperation application.

REFERENCES

Akahane, K., S. Hasegawa, Y. Koike, and M. Sato. 2005. A Development of High Definition Haptic Controller. *First Joint Eurohaptics Conference and Symposium on Haptic Interfaces for Virtual Environment and Teleoperator Systems.*

Benali-Khoudja, M., M. Hafez, and A. Kheddar. 2007. VITAL: An electromagnetic integrated tactile display. *Displays* 28:133–144.

Berkelman, P.J., R.L. Hollis, and S.E. Salcudean. 1995. Interacting with Virtual Environments using a Magnetic Levitation Haptic Interface. *IEEE 1995.*

Birglen, L., C. Gosselin, N. Pouliot, B. Monsarrat, and T. Laliberté. 2002. SHaDe, A New 3-DOF Haptic Device. *IEEE Transactions On Robotics and Automation* 18:2.

Boian, R., F. Deutsch, J., F. Chan Su Lee Burdea, G., C. and J, Lewis. 2003. Haptic effects for virtual reality-based post-stroke rehabilitation. *IEEE Haptic Interfaces for Virtual Environment and Teleoperator Systems, 2003. HAPTICS.* 247-253.

Bowen, K., and M. K. O'Malley. 2006. Adaptation of Haptic Interfaces for a LabVIEW-based System Dynamics Course. *Symposium on Haptic Interfaces for Virtual Environment and Teleoperator Systems 2006 March 25 - 26, Alexandria, Virginia, USA.*

Cao, Y., Y. Zhang, Y. Ma, and D. Wang. 2007. Design and Analysis of a New Six-DOF Haptic Device for Dental Training. *16th IEEE International Conference on Robot & Human Interactive Communication August 26 - 29, 2007, Jeju, Korea.*

Carlbom, I., and Paciorek J. 1978. Planar Geometric Projections and Viewing Transformations. *ACM Computing Surveys* 10(4):465–502.

Carignan, C., J. Tang, and S. Roderick. 2009. Development of an Exoskeleton Haptic Interface for Virtual Task Training. *The 2009 IEEE/RSJ International Conference on Intelligent Robots and Systems October 11-15, 2009 St. Louis, USA.*

Choi B. H., and H. R. Choi. 1999. A Semi-direct Drive Hand Exoskeleton Using Ultrasonic Motor. *IEEE International Workshop on Robot and Human Interaction Pisa, Italy - September 1999.*

Dachille, F., H. Qin, and A. Kaufman. 2001. A novel haptics-based interface and sculpting system for physics-based geometric design. *Computer-Aided Design* 33:403-420.

Dede, M., I., C.O. Selvi, T. Bilgincan, Y. Kant. 2009. Design of a haptic device for teleoperation and virtual reality systems. *IEEE International Conference on* Systems, *Man and Cybernetics.* 3623 - 3628

Faulring, E.L., J.E. Colgate, and M.A. Peshkin. 2004. A High Performance 6-DOF Haptic Cobot. *IEEE International Conference on Robotics and Automation*, 2004.

Force Dimension Official WEB site. www.forcedimension.com (accessed April, 2010)

Frisoli, A., F. Simoncini, M. Bergamasco, and F. Salsedo. 2007. Kinematic Design of a Two Contact Points Haptic Interface for the Thumb and Index Fingers of the Hand. *Journal of Mechanical Design* 129:520.

Gallina, P., and G. Rosati. 2002. Manipulability of a planar wire driven haptic device. *Mechanism and Machine Theory* 37:215-228.

Gosline, A.H.C., and V. Hayward. 2008. Eddy Current Brakes for Haptic Interfaces: Design, Identification, and Control. *IEEE/ASME Transactions On Mechatronics* 13:6.

Gosselin, F., J.P. Martins, C. Bidard, C. Andriot, and J. Brisset. 2005. Design of a New Parallel Haptic Device for Desktop Applications. *First Joint Eurohaptics Conference and Symposium on Haptic Interfaces for Virtual Environment and Teleoperator Systems 2005.*

Hara, M., G. Matthey, and A. Yamamoto. 2009. Development of a 2-DOF Electrostatic Haptic Joystick for MRI/fMRI Applications. *IEEE International Conference on Robotics and Automation Kobe International Conference Center Kobe, Japan, May 12-17, 2009.*

He, X., and Y. Chen. 2008. Haptic-aided robot path planning based on virtual tele-operation *Robotics and Computer-Integrated Manufacturing, 2008.*

Hirabayashi, T., J. Akizono, T. Yamamoto, H. Sakai, and H. Yano. 2006. Teleoperation of construction machines with haptic information for underwater applications. *Automation in Construction* 15:563 – 570.

Horan, B., D. Creighton, S. Nahavandi, and M. Jamshidi. 2007. Bilateral haptic teleoperation of an articulated track mobile robot. *IEEE International Conference on System of Systems Engineering, 2007. SoSE '07* 1 – 8.

Directindustry International industrial machine part supplier. www.directindustry.com (accessed April, 2010).

Honeywell International Official WEB site. http://www.honeywell.com/ (accessed May, 2010)

Jairakrean, S., and T. Chanthasopeephan. 2009. Position Control of SMA Actuator for 3D Tactile Display. *IEEE 11th International Conference on Rehabilitation Robotics Kyoto International Conference Center, Japan, June 23-26, 2009.*

Jobin, M., R. Foschia, S. Grange, C. Baur, G. Gremaud, K. Lee, L. Forró, and A. Kulik. 2005. Versatile force–feedback manipulator for nanotechnology applications. *Review of Scientific Instruments* 76:053701.

Kayyalil, R., S. Shirmohammadil, and A. El Saddik. 2008. Measurement of Progress for Haptic Motor Rehabilitation Patients. *IEEE International Workshop on Medical Measurements and Applications* 108:113.

Khanicheh, A., D. Mintzopoulos, B. Weinberg, A.A. Tzika, and C. Mavroidis. 2008. MR_CHIROD v.2: Magnetic Resonance Compatible Smart Hand Rehabilitation Device for Brain Imaging. *IEEE Transactions On Neural Systems and Rehabilitation Engineering* 16:1.

Kikuchi, T., H. Xinghao, K. Fukushima, K. Oda, J. Furusho, and A. Inoue. 2007. Quasi-3-DOF Rehabilitation System for Upper Limbs: Its Force-Feedback Mechanism and Software for Rehabilitation. *IEEE 10th International Conference on Rehabilitation Robotics, June 12-15, Noordwijk, The Netherlands.*

Kim, J.W., D.H. Park, H.S. Kim, and S.H. Han. 2007. Design of a Novel 3-DOF Parallel-type Haptic Device with Redundant Actuation. *International Conference on Control, Automation and Systems 2007 Oct. 17-20, 2007 in COEX, Seoul, Korea.*

Kim, K., W. K. Chung , and Y. Youm. 2003. Design and Analysis of a New 7-DOF Parallel Type Haptic Device : PATHOS-I1. *Conference on Intelligent Robots and Systems Las Vegas. Nevada October 2003.*

Kyung, K.U., J.Y. Lee, and J. Park. 2007. Design and Applications of a Pen-Like Haptic Interface with Texture and Vibrotactile Display. *Frontiers in the Convergence of Bioscience and Information Technologies 2007.*

Labjack Company, Inc Official WEB site. labjack.com (accessed April, 2010)

Lee, S., G.S. Sukhatme, G. J. Kim, and C.M. Park. 2005. Haptic Teleoperation of a Mobile Robot: A User Study. *Presence Teleoperators and Virtual Environments 14* 3: 345-365,

Lee, J.H., K.S. Eom, B.J. Yi, and I. H. Suh. 2001. Design Of A New 6-DOF Parallel Haptic Device. *IEEE International Conference on Robotics & Automation Seoul, Korea, May 21-26, 2001.*

Lee, J., S.N. Sponberg, O.Y. Loh, A.G. Lamperski, R.J. Full, and N.J. Cowan. 2008. Templates and Anchors for Antenna-Based Wall Following in Cockroaches and Robots. *IEEE Transactions On Robotics* 24:1.

Lee, S.S., and J.M. Lee. 2003. Design of a general purpose 6-DOF haptic interface. *Mechatronics* 13:697–722.

Lelieveld, M.J., and T. Maeno. 2006. Design and Development of a 4 DOF Portable Haptic Interface with Multi-Point Passive Force Feedback for the Index Finger. *IEEE International Conference on Robotics and Automation Orlando, Florida - May 2006.*

Li, W.H., B. Liu, P.B. Kosasih, and X.Z. Zhang. 2007. A 2-DOF MR actuator joystick for virtual reality applications. *Sensors and Actuators A* 137:308–320.

Mali, U., and M. Munih. 2003. Real-time control of haptic device using personal computer. *EUROCON 2003 Ljubljana Slovenia.*

Massie, T.H., and J.K. Salisbury. 1994. The PHANTOM Haptic Interface: A Device for Probing Virtual Objects. *ASME Winter Annual Meeting, Symposium on Haptic Interfaces for Virtual Environment and Teleoperator Systems, Chicago, IL, Nov. 1994.*

Medical Source about drugs and diseases. www.medical-look.com (accessed April, 2010)

National Instruments Official WEB site. www.ni.com (accessed April, 2010)

Novint Technologies, Inc Official WEB site. http://home.novint.com (accessed April, 2010)

Okada, J., and Y. Toh. 2004. Antennal system in cockroaches: a biological model of active tactile sensing. *International Congress Series* 1269:57– 60.

Park, K., B. Bae, and T. Koo. 2004. A haptic device for PC video game application. *Mechatronics* 14:227–235.

Payeur, P., C. Pasca, A.M., Cretu, and E.M. Petriu. 2005. Intelligent Haptic Sensor System for Robotic Manipulation. *IEEE Transactions On Instrumentations and Measurement* 54:4.

Peer A., and M. Buss. 2008. A New Admittance-Type Haptic Interface for Bimanual Manipulations. *IEEE/ASME Transactions On Mechatronics* 13:4.

Quanser Consulting Inc. Official WEB site. www.quanser.com (accessed April, 2010)

Ryu, D., J.B. Song, C. Cho, S. Kang, and M. Kim. 2009. Development of a six DOF haptic master for teleoperation of a mobile manipulator. *Mechatronics 2009*.

Sabater A, J.M., R.J. Saltarén, and R. Aracil. 2004. Design, modelling and implementation of a 6 URS parallel haptic device. *Robotics and Autonomous Systems* 47:1–10.

Samur E., L. Flaction, U. Spaelter, and H. Bleuler. 2008. A Haptic Interface with Motor/Brake System for Colonoscopy Simulation *Symposium on Haptic Interfaces for Virtual Environment and Teleoperator Systems 2008 13-14 March, Reno, Nevada, USA*

Schosteka, S., M.O. Schurra, and G.F. Buessb. 2009. Review on aspects of artificial tactile feedback in laparoscopic surgery. *Medical Engineering & Physi*cs 31:887–898.

Schwerdt, H.N., J. Tapson, and R. E. Cummings. 2009. A Color Detection Glove with Haptic Feedback for the Visually Disabled. *IEEE 2009.*

Sensable Technologies, Inc Official WEB site. www.sensable.com (accessed April, 2010)

Smid, G.E., and C. Melchiorri. 1998. Real-Time Control for VIDET using Simulink. *IEEE 1998.*

Sone, J., R. Inoue, K. Yamada, T. Nagae, K. Fujita, and M. Sato. 2008. Development of a Wearable Exoskeleton Haptic Interface Device. *Journal of Computing and Information Science in Engineering* 8:041009-1.

Takaiwa M., and T. Noritsugu. 1999. Application of Pneumatic Parallel Manipulator as Haptic Human Interface. *IEEE/ASME International Conference on Advanced Intelligent Mechatronics September 19-23, 1999 Atlanta, USA.*

Tanner, N.A., and G Niemeyer. 2006. High-Frequency Acceleration Feedback in Wave Variable Telerobotics. *IEEE/ASME Transactions on Mechatronics* 11:119-127.

Taylor, P.M., A. Moser, and A. Creed. 1998. A Sixty-Four Element Tactile Display Using Shape Memory Alloy Wires. *Displays* 18:163-168.

Salonix Technical service provider about pneumatics and automation. www.salonix.md. (accessed April, 2010)

Tsagarakis, N., D.G.Caldwell, and G.A.M. Cerda. 1999. A 7 dof pneumatic Muscle Actuator (pMA) powered Exoskeleton. *IEEE International Workshop on Robot and Human Interaction Pisa, Italy - September 1999.*

Uchiyama, M., Y. Tsumaki, and W.K. Yoon. 2007. Design of a Compact 6-DOF Haptic Device to Use Parallel Mechanisms. *Robotics Research Star* 28:145-162.

Vlachos, K., E. Papadopoulos, and D.N. Mitropoulos. 2003. Design and Implementation of a Haptic Device for Training in Urological Operations. *IEEE Transactions On Robotics and Automation* 19:5.

Vlachos, K., and E. Papadopoulos. 2008. Analysis and Experiments of a Haptic Telemanipulation Environment for a Microrobot Driven by Centripetal Forces. *Journal of Computing and Information Science in Engineering* 8:041007-1.

Wang, P., A.A. Becker,, I.A. Jones, A.T. Glover, S.D. Benford, C.M. Greenhalgh,and M. Vloeberghs. 2006. A virtual reality surgery simulation of cutting and retraction in neurosurgery with force-feedback. *Computer Methods and Programs in Biomedicine* 84:11-18.

Yoon, J., and J. Ryu. 2001. Design, Fabrication, and Evaluation of a New Haptic Device Using a Parallel Mechanis. *IEEE/ASME Transactions On Mechatronics* 6:3.

Zitzewitz J.V., G. Rauter, A. Brunschweiler, and R. Riener. 2008. Hybrid actuation concepts for a rope robot as a haptic interface. *IEEE/RAS-EMBS International Conference on Biomedical Robotics and Biomechatronics Scottsdale, AZ, USA, October 19-22, 2008.*

APPENDIX A

SOURCE CODES OF THE SYSTEM

A.1. Source Code of ADC to DAC Converter

```
/*********************************************************
     3 Channels ADC to DAC Converter
*********************************************************/

#include <16f877A.h>     \\ Microprocessor configurations
#fusesHS,WDT,PROTECT,NOBROWNOUT,NOLVP,NOPUT,NOWRT,
NODEBUG, CPD
#use delay (clock=10000000)

unsigned int16  Value=0;     \\ Global variables
#include "DAC714_4.c"     \\ Included library
#include "ADS8320_C.c"


/*********Main Program Functions********/

void main ( )
{

  setup_psp(PSP_DISABLED);     \\ Internal interrupts
  setup_spi(SPI_SS_DISABLED);
  setup_timer_1(T1_DISABLED);
  setup_timer_2(T2_DISABLED,0,1);
  setup_adc_ports(NO_ANALOGS);
  setup_adc(ADC_OFF);
  setup_CCP1(CCP_OFF);
  setup_CCP2(CCP_OFF);
  setup_wdt(wdt_2304ms);
  disable_interrupts(GLOBAL);

-------------------------------------

  init_ext_adc_C(pin_d2, pin_d3, pin_c4);     \\ Initializing the converters
  init_ext_adc_C(pin_c5, pin_c6, pin_c7);
  init_ext_adc_C(pin_d4, pin_d5, pin_d6);
  init_DAC714(pin_d1, pin_d0, pin_c3, pin_c2);
  init_DAC714(pin_c1 pin_c0, pin_e2, pin_e1);
  init_DAC714(pin_e0, pin_a5, pin_a4, pin_a3);
```

```
while(True)
  {

  value=read_ext_adc_C(pin_d2, pin_c4, pin_d3);     \\ Converting data
  DAC_Write16(Value,pin_d1, pin_d0, pin_c3, pin_c2);
  output_low(pin_b7);

  value=read_ext_adc_C(pin_c5, pin_c6, pin_c7);
  DAC_Write16(Value,pin_c1 pin_c0, pin_e2, pin_e1);
  output_low(pin_b7);

  value=read_ext_adc_C(pin_d4, pin_d5, pin_d6);
  DAC_Write16(Value,pin_e0, pin_a5, pin_a4, pin_a3);
  output_low(pin_b7);


  }
}
```

A.2. Source Code of Computer Control and Virtual Reality Software

The computer control and VR software of the system is developed in Matlab Simulink via Quanser Q8 analog inputs. Each operation for the control of the impedance type haptic device is conducted in separate matlab blocks. The blocks that are configured for VR application, sensor readings, forward kinematics and force calculation can be seen in the main window of the software (Figure A.1).

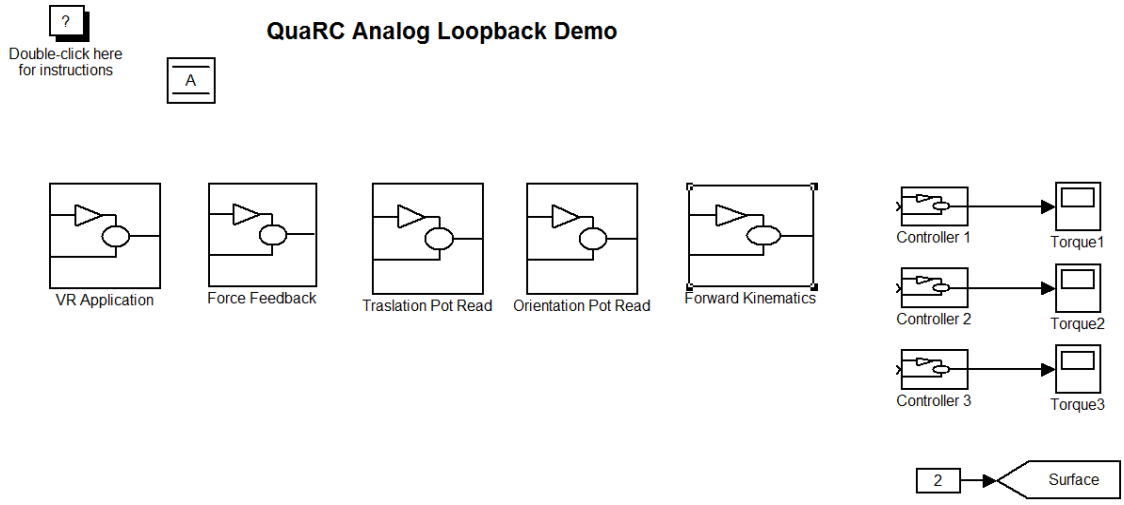

Figure A.1. Main program

The initial tests of the mechanism and the actuators are performed as a conventional manipulator then the system is operated as haptic system. The tests of the system is executed by making use of the control blocks which can be observed in Figure A.1 with controller 1, 2, 3.

The positions of the links are measured through the potentiometers with HIL Read Analog block then the readings are adjusted as shown in Figure A.2. The first math block sets the zero position of the links and the multiplication operations converts the ±10v analog inputs to degrees.

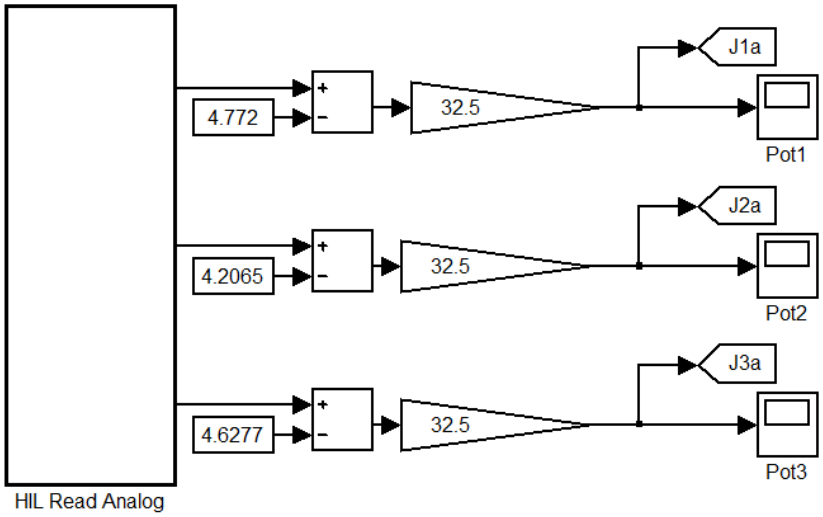

Figure A.2. Translation mechanism Pot Read Block

Similar to the translation mechanism, position angles of the orientation mechanism's links are calculated with similar math operations as shown in Figure A.3.

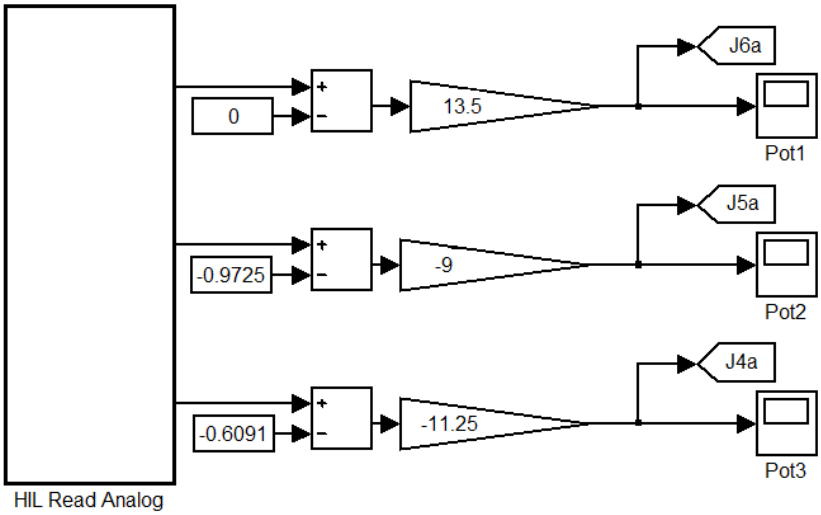

Figure A.3. Orientation mechanism Pot Read Block

The forward kinematic calculation of the translation mechanism is solved in forward kinematics block which can be seen in Figure A.4. The calculation translates the link angles to position of the Wr point.

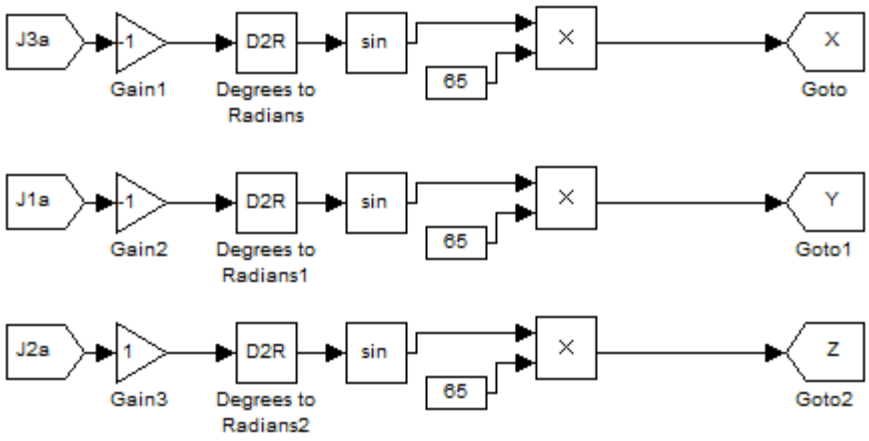

Figure A.4. Forward kinematics block

The VR application is created with VR sink block in simulink (Figure A.5) and connected with the position of the Wr point. The VR application is a basic pen and surface application (Figure A.6) which can simulate point type of contact in 6-DOF space.

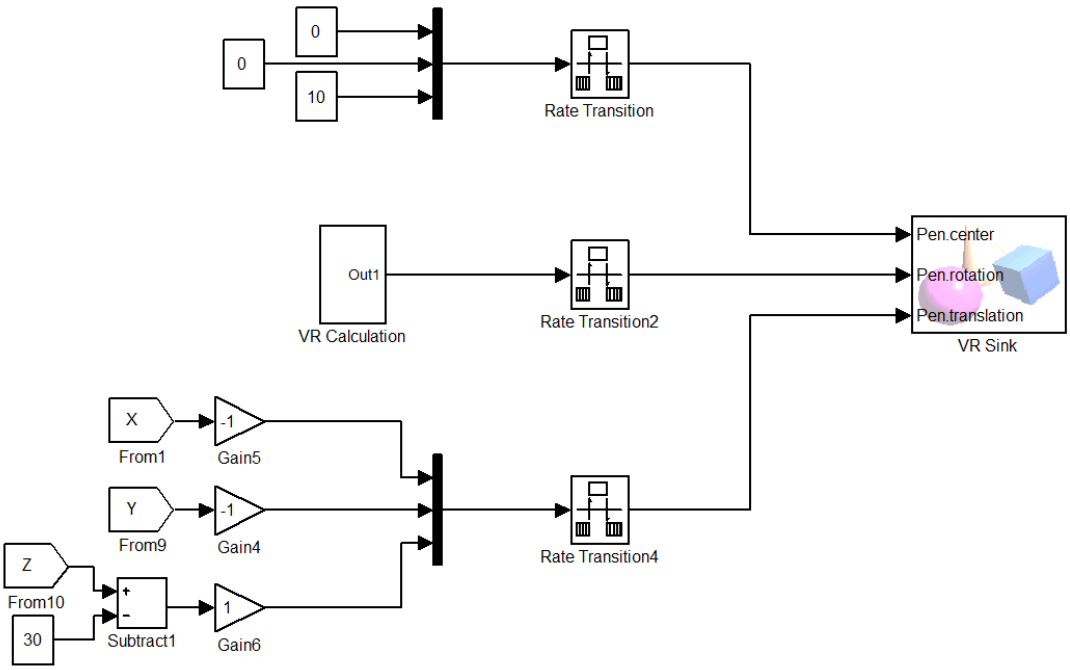

Figure A.5.VR application block

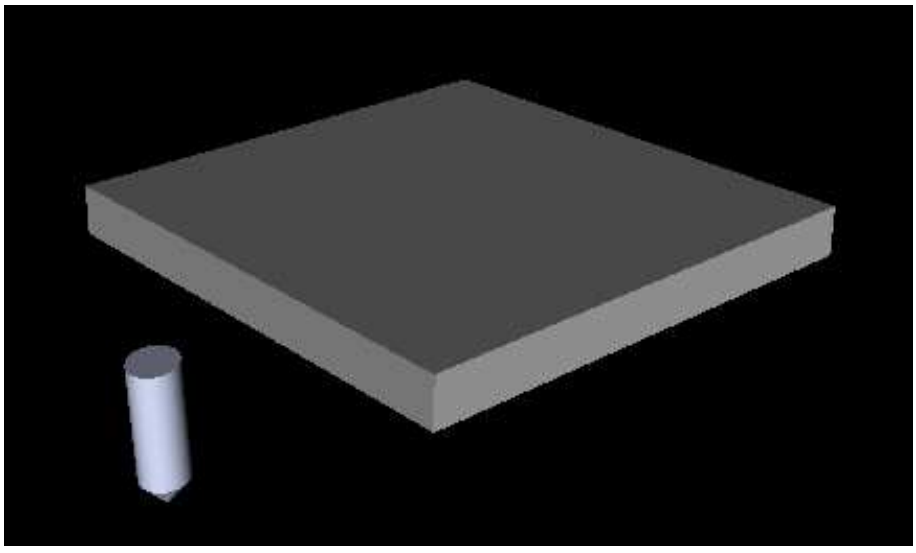

Figure A.6. VR application

Finally the VR haptic surface is determined in force feedback block and the calculated torqueses are applied to the user via HIL Analog Write block as shown in Figure A.7.

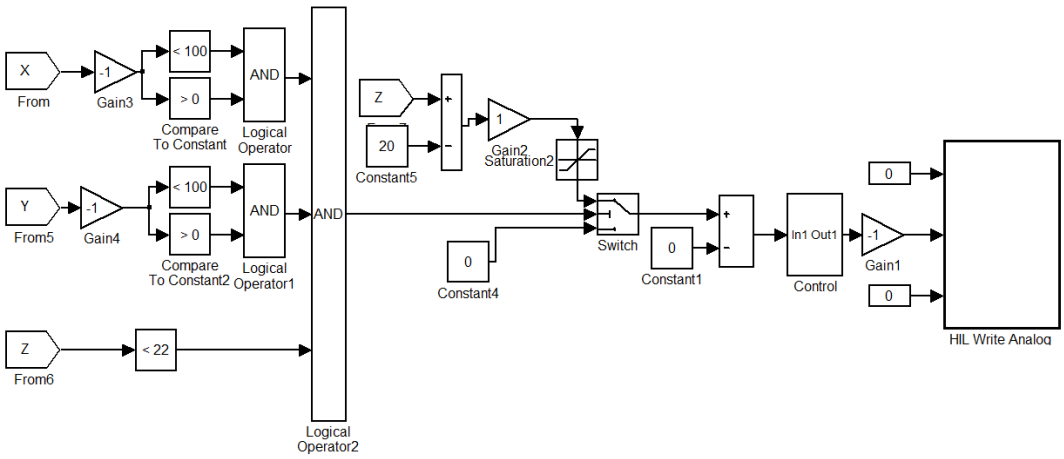

Figure A.7. Force feedback block

APPENDIX B

ISOMETRIC VIEWS AND PROPERTIES OF THE LINKS

B.1. Translation Mechanism

Table B.1. Translation mechanism Link1

Density	Mass	Volume	Surface Area
0.0028 g/mm³	16.96 grams	6055.82 mm^3	3784.83 mm^2

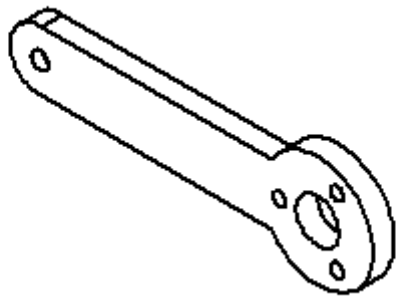

Figure B.1. Translation mechanism Link1

Table B.2. Translation mechanism Link2

Density	Mass	Volume	Surface Area
0.0028 g/mm³	54.21 grams	19361.66 mm^3	12594.63 mm^2

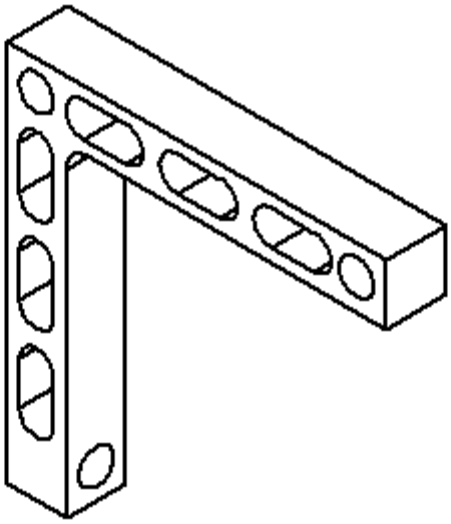

Figure B.2. Translation mechanism Link2

Table B.3. Translation mechanism Link3

Density	Mass	Volume	Surface Area
0.0028 g/mm³	22.02 grams	7863.40mm^3	4558.67 mm^2

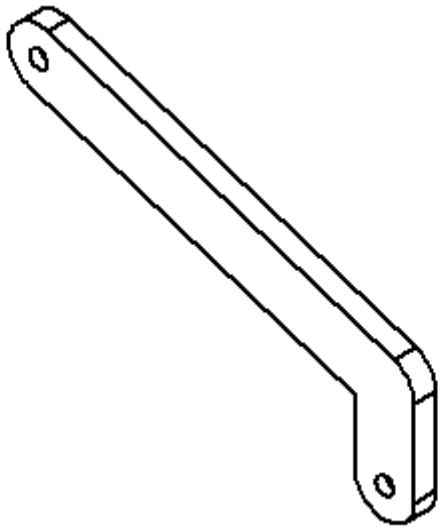

Figure B.3. Translation mechanism Link3

Table B.4. Translation mechanism Link4

Density	Mass	Volume	Surface Area
0.0028 g/mm³	60.93 grams	21761.05 mm^3	13751.85 mm^2

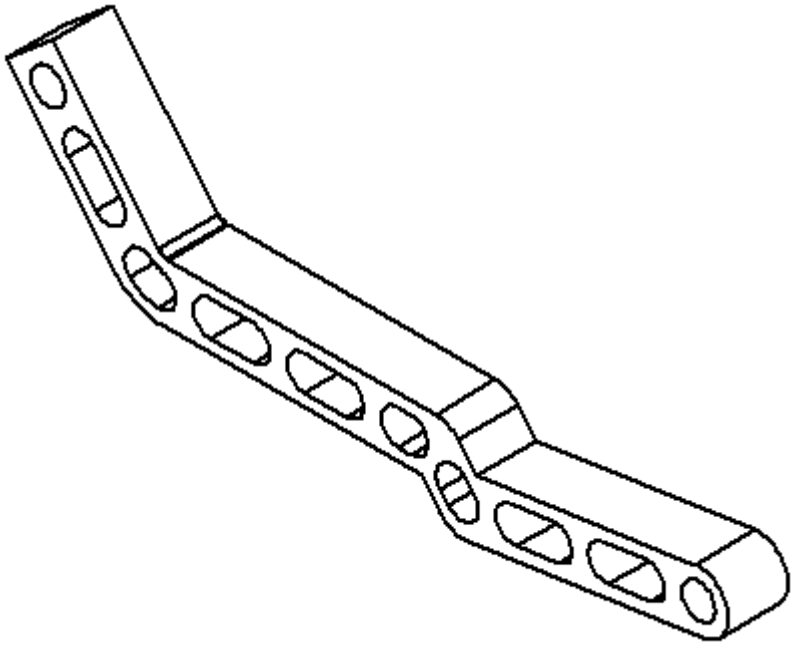

Figure B.4. Translation mechanism Link4

Table B.5. Translation mechanism Link5

Density	Mass	Volume	Surface Area
0.0028 g/mm³	71.30 grams	51297.53 mm^3	15203.87 mm^2

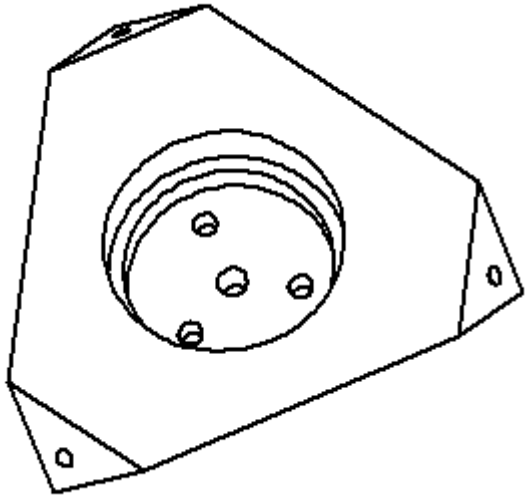

Figure B.5. Translation mechanism Link5

B.2. Orientation Mechanism

Table B.6. Orientation mechanism Link1

Density	Mass	Volume	Surface Area
0.0014 g/mm³	19.43 grams	13977.54 mm3	6680.48 mm2

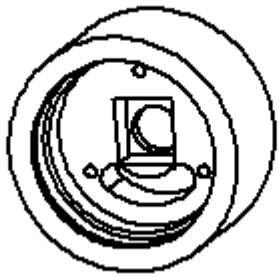

Figure B.6. Orientation mechanism Link1

Table B.7. Orientation mechanism Link2

Density	Mass	Volume	Surface Area
0.0014 g/mm³	18.72 grams	13467.72 mm3	7302.14 mm2

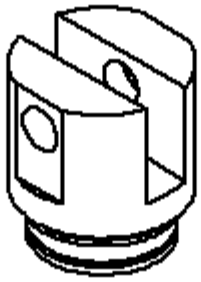

Figure B.7. Orientation mechanism Link2

Table B.8. Orientation mechanism Link3

Density	Mass	Volume	Surface Area
0.0014 g/mm³	10.71 grams	7705.32 mm3	5259.06 mm2

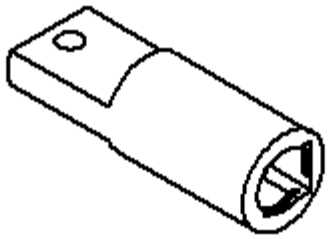

Figure B.8. Orientation mechanism Link3

Table B.9. Orientation mechanism Link4

Density	Mass	Volume	Surface Area
0.0014 g/mm³	47.17 grams	33935.26 mm3	11310.36 mm2

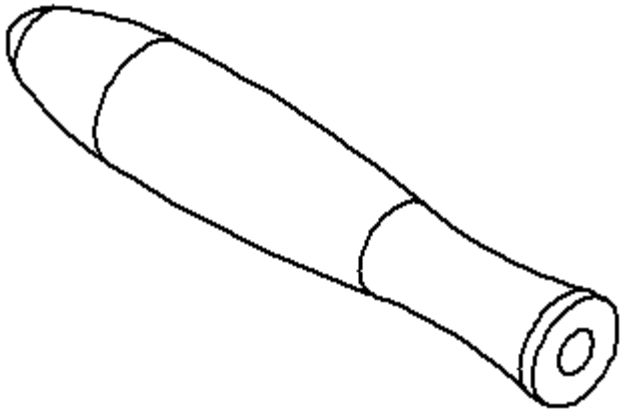

Figure B.9. Orientation mechanism Link4